USGS
science for a changing world

هيئة المساحة الجيولوجية السعودية
SAUDI GEOLOGICAL SURVEY

Paleomagnetism of the Harrat Rahat Volcanic Field, Kingdom of Saudi Arabia—Geologic Unit Correlations and Geomagnetic Cryptochron Identifications

Chapter H of
Active Volcanism on the Arabian Shield—Geology, Volcanology, and Geophysics of Northern Harrat Rahat and Vicinity, Kingdom of Saudi Arabia

U.S. Geological Survey Professional Paper 1862
Saudi Geological Survey Special Report SGS–SP–2021–1

U.S. Department of the Interior
U.S. Geological Survey

Cover. Photograph looking south-southeast at the Al Du'aythah cinder cones located 13 kilometers west-southwest of the center of Al Madīnah. Peak on left skyline is Jabal aş Şu'lūk composed of Precambrian rocks. Flat-topped peak in distant center skyline is Jabal al Asmar consisting of Precambrian rocks capped by Miocene alkali basalt. U.S. Geological Survey photograph by Gail Mahood, February 24, 2014. Background image shows northern Harrat Rahat lava flows, maars, and lava domes. U.S. Geological Survey photograph by Andrew Calvert, January 25, 2012.

Paleomagnetism of the Harrat Rahat Volcanic Field, Kingdom of Saudi Arabia—Geologic Unit Correlations and Geomagnetic Cryptochron Identifications

By Duane E. Champion, Drew T. Downs, Mark E. Stelten, Joel E. Robinson, Thomas W. Sisson, Jamal Shawali, Khalid Hassan, and Hani M. Zahran

Chapter H of

Active Volcanism on the Arabian Shield—Geology, Volcanology, and Geophysics of Northern Harrat Rahat and Vicinity, Kingdom of Saudi Arabia

Edited by Thomas W. Sisson, Andrew T. Calvert, and Walter D. Mooney

U.S. Geological Survey Professional Paper 1862
Saudi Geological Survey Special Report SGS–SP–2021–1

U.S. Department of the Interior
U.S. Geological Survey

U.S. Geological Survey, Reston, Virginia: 2023

For more information on the USGS—the Federal source for science about the Earth, its natural and living resources, natural hazards, and the environment—visit https://www.usgs.gov or call 1–888–ASK–USGS.

For an overview of USGS information products, including maps, imagery, and publications, visit https://store.usgs.gov.

Suggested citation:
Champion, D.E., Downs, D.T., Stelten, M.E., Robinson, J.E., Sisson, T.W., Shawali, J., Hassan, K., and Zahran, H.M., 2023, Paleomagnetism of the Harrat Rahat volcanic field, Kingdom of Saudi Arabia—Geologic unit correlations and geomagnetic cryptochron identifications, chap. H *of* Sisson, T.W., Calvert, A.T., and Mooney, W.D., eds., Active volcanism on the Arabian Shield—Geology, volcanology, and geophysics of northern Harrat Rahat and vicinity, Kingdom of Saudi Arabia: U.S. Geological Survey Professional Paper 1862 [also released as Saudi Geological Survey Special Report SGS–SP–2021–1], 31 p., https://doi.org/10.3133/pp1862H.

ISSN 1044-9612 (print)
ISSN 2330-7102 (online)

هيئة المساحة الجيولوجية السعودية
SAUDI GEOLOGICAL SURVEY

Ministry of Industry and Mineral Resources
BANDAR BIN IBRAHIM BIN ABDULLAH AL-KHORAYEF, Minister and SGS Chairman

Saudi Geological Survey
Abdullah bin Mufter Al-Shamrani, Chief Executive Officer

Saudi Geological Survey, Jiddah, Kingdom of Saudi Arabia: 2023

Contents

Abstract....1
Introduction....1
Methods....3
$^{40}Ar/^{39}Ar$ Dating....14
^{36}Cl Cosmogenic Surface-Exposure Dating....14
Results....14
Historical 1256 C.E. (654 A.H.) Flow....14
641 C.E. (20 A.H.) Eruption....18
Five Fingers Lava Flows....21
Lava Flows within Al Madīnah....21
Identifying Brief Eruptive Episodes in Harrat Rahat....21
Geomagnetic Excursions Recorded at Harrat Rahat....24
Conclusions....28
Acknowledgments....28
References Cited....29

Figures

1. Map of the Kingdom of Saudi Arabia and the surrounding region....2
2. Geologic map of northern Harrat Rahat showing the locations of paleomagnetic core sampling....4
3. Northern part of a lower hemisphere equal-area plot showing mean directions of remanent magnetization with enclosing 95 percent uncertainties for sampled sites in Harrat Rahat....16
4. Plot of archaeomagnetic inclinations and declinations spanning the past 8,000 years from Bulgaria compared to the remanent magnetic direction for the historical basalt of Al Labah....17
5. Plot of archaeomagnetic inclinations and declinations spanning the past 8,000 years from Bulgaria compared to the remanent magnetic direction for the basalt of Al Du'aythah....19

6. Plot of archaeomagnetic inclinations and declinations spanning the past 8,000 years from Bulgaria compared to the remanent magnetic direction for the Habir basalt flow of Harrat Khaybar 20
7. Northern part of lower hemisphere equal-area plots showing site mean directions of remanent magnetization and enclosing 95 percent confidence envelopes for sites thought to have erupted penecontemporaneously as determined from their locations, geologic field relations, geochronology, and similar magnetizations 23
8. An equal-area plot showing site mean directions of remanent magnetization and enclosing 95 percent confidence envelopes for sites showing anomalous character outside the range of ordinary secular variation 25
9. Northern part of a lower hemisphere equal-area plot showing site mean directions of remanent magnetization and enclosing 95 percent confidence envelopes for sites thought to record sweeping changes in the local magnetic field acquired during the Iceland Basin Cryptochron 26

Tables

1. Paleomagnetic results from sites in northern Harrat Rahat and additional sites in Harrats Khaybar and Ithnayn 5
2. List of mapped geologic units grouped based on close or overlapping $^{40}Ar/^{39}Ar$ or ^{36}Cl ages and similar paleomagnetic directions 15
3. Summary of new $^{40}Ar/^{39}Ar$ ages for three Harrat Rahat lava flows 26

Conversion Factors

International System of Units to U.S. customary units

Multiply	By	To obtain
	Length	
centimeter (cm)	0.3937	inch (in.)
millimeter (mm)	0.03937	inch (in.)
meter (m)	3.281	foot (ft)
kilometer (km)	0.6214	mile (mi)
kilometer (km)	0.5400	mile, nautical (nmi)
meter (m)	1.094	yard (yd)
	Area	
square kilometer (km^2)	247.1	acre
square kilometer (km^2)	0.3861	square mile (mi^2)
	Volume	
cubic kilometer (km^3)	0.2399	cubic mile (mi^3)

Temperature in degrees Celsius (°C) may be converted to degrees Fahrenheit (°F) as follows:

$$°F = (1.8 \times °C) + 32.$$

Datum

Vertical coordinate information is referenced to the World Geodetic System of 1984 (WGS 1984).

Abbreviations

AF	alternating field
A.H.	in year of the Hijra
C.E.	Common Era
IRM	isothermal remanent magnetization
ka	kilo-annum
TRM	thermoremanent magnetization
VGP	virtual geomagnetic pole
σ	standard deviation

Active Volcanism on the Arabian Shield
Edited by T.W. Sisson, A.T. Calvert, and W.D. Mooney
U.S. Geological Survey Professional Paper 1862
Saudi Geological Survey Special Report SGS–SP–2021–1

Chapter H

Paleomagnetism of the Harrat Rahat Volcanic Field, Kingdom of Saudi Arabia—Geologic Unit Correlations and Geomagnetic Cryptochron Identifications

By Duane E. Champion,[1] Drew T. Downs,[2] Mark E. Stelten,[2] Joel E. Robinson,[2] Thomas W. Sisson,[2] Jamal Shawali,[3] Khalid Hassan,[3] and Hani M. Zahran[3]

Abstract

Paleomagnetic rock samples were collected from 173 drill sites in the Quaternary alkali basaltic volcanic field of northern Harrat Rahat, Kingdom of Saudi Arabia. Laboratory measurements on these samples established that lava flows and vent complexes—identified and mapped from field characteristics, rock types, and compositions as products of single or temporally close eruptions—typically record single, or very similar, directions of remanent magnetization. Correlations defined through geologic mapping, spatial association, geochemistry, geochronology, and identical mean remanent directions indicate at least 16 brief episodes of temporally clustered eruptions. These episodes had durations of a few centuries or less. Anomalous remanent magnetic directions were found for at least 13 mapped lavas of northern Harrat Rahat, which demonstrate that they were acquired during brief geomagnetic cryptochrons during the Brunhes Normal Polarity Chron. These uncharacteristic directions enhance the opportunity to identify common eruptive episodes, and to better understand and evaluate assessments of eruption ages based on $^{40}Ar/^{39}Ar$ geochronology. Combining paleomagnetic and regional archaeomagnetic results for the youngest eruptions allows us to evaluate their historical age assignments and, in one case, refute a previously assigned provisional age.

Introduction

Paleomagnetic field studies were undertaken within the northern part of the Quaternary Harrat Rahat volcanic field in the Kingdom of Saudi Arabia to aid in correlating lava flows and other volcanic deposits and to refine understanding of the timing and duration of eruptive episodes based on $^{40}Ar/^{39}Ar$ geochronology (fig. 1). We found that agreement of recorded directions of remanent magnetization in the Harrat Rahat lava flows, which are predominately of mafic compositions, with the guidance of geologic field relations, whole-rock major oxide and trace element compositions, and radiometric ages ($^{40}Ar/^{39}Ar$ and ^{36}Cl methods) best establishes the brevity of individual volcanic eruptive events. These intervals are paleomagnetically defined as less than a century, but global historical eruptive activity shows that the actual eruptive durations can last only months, years, or decades. The well documented historical eruption of the basalt of Al Labah in 1256 C.E. (654 in the year of the Hijra [A.H.]), adjacent to the city of Al Madīnah al Munawwarah, which lasted only 52 days and produced 0.5 cubic kilometers (km^3) of lava (Al-Samhūdī, 1488; Camp and others, 1987), is an example of a brief but voluminous basaltic eruptive episode.

The original constructional morphology of the lava flows within the urbanized portions of Al Madīnah has been extensively modified by millennia of building by city inhabitants, making conventional geologic mapping difficult. Remanent magnetic directions measured for outcrops along streets and among buildings were essential aids to correlate or distinguish lava flows. Groups of similar mean remanent magnetic directions were an important guide to the extent and number of separate eruptions that produced lava flows that entered what is now the present area of the city.

Mean directions of remanent magnetization, from one or more sites located within a lava deposit, establish the local orientation of the geomagnetic field at the time of that brief eruption. Directions from different eruptive units (lava flows, flow lobes, vent complexes, some tuffs, or scoria), if similar, can suggest brief episodes wherein magma erupted from multiple vent sites, lasting no more than a century or two as revealed by the stratigraphy and geochronology of those units. In doing so, we find 16 unit-to-unit remanent direction correlations within northern Harrat Rahat lava flows during the Brunhes Normal Polarity Chron (780 thousand years ago [ka] to present).

[1]U.S. Geological Survey, now deceased.

[2]U.S. Geological Survey.

[3]Saudi Geological Survey.

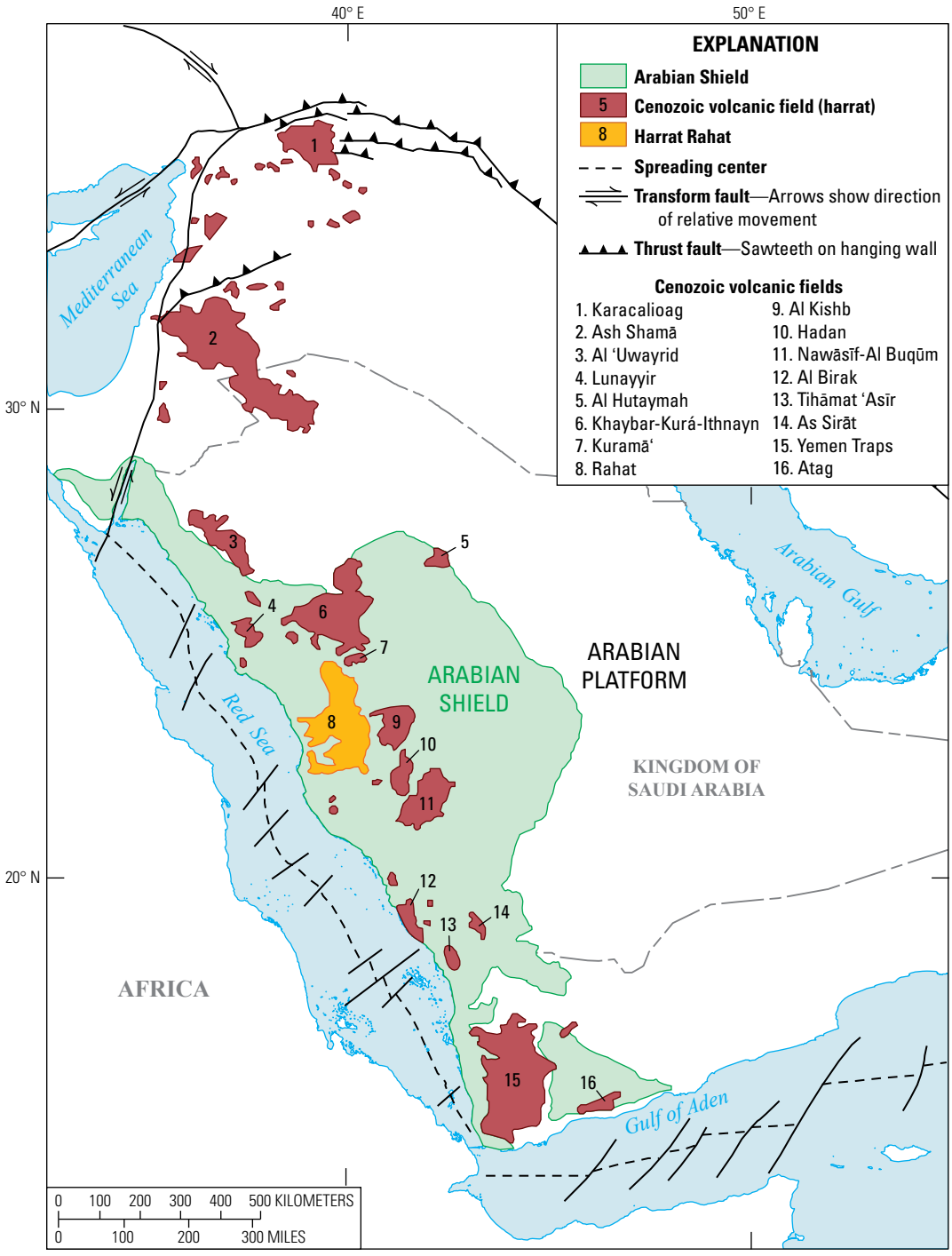

Figure 1. Map of the Kingdom of Saudi Arabia and the surrounding region. Red areas mark the locations of Cenozoic volcanic fields of the Arabia Plate. Harrat Rahat is shown in orange. The Arabian Shield (green) is a region of exposed Neoproterozoic (meta)igneous and (meta)sedimentary rocks. The Arabian Platform (uncolored) consists of flat-lying to gently east-dipping Phanerozoic sedimentary rocks and surficial unconsolidated sediments. Major tectonic features were compiled by Stern and Johnson (2010) from prior publications. Locations of Cenozoic volcanic fields are from Coleman and others (1983) and Camp and Roobol (1989). Cenozoic volcanic rocks and other geologic and tectonic features are omitted west of the Red Sea and south of the Gulf of Aden.

Mean directions of magnetization established for the young-appearing lava flows and vent complexes of northern Harrat Rahat were used to independently estimate their eruptive ages by comparison to regional records of geomagnetic variation with time. These directions were compared to the closest, most continuous record of local magnetic variation established for Bulgaria by Kovacheva and others (2009) from archaeomagnetic data. The comparison with the remanent direction from the historically described basalt of Al Labah successfully matches its known age of 1256 C.E. (654 A.H.). However, another comparison with the remanent direction from four small cones of the basalt of Al Du'aythah, near the intersection of King Khalid and King Saud Roads in Al Madīnah's western suburbs, is shown to not match the age of 641 C.E. (20 A.H.). This age was provisionally assigned by Camp and Roobol (1989) and Murcia and others (2015) based on the rocks' young appearance and a brief historical note (Al-Samhūdī, 1488) of an eruption somewhere in the greater Al Madīnah region in that year. An age derived from ^{36}Cl cosmogenic surface-exposure dating indicates that the basalt of Al Du'aythah erupted at ~13 ka. Instead, we show that mean remanent directions from sites in the voluminous basaltic Habir lava flow of Harrat Khaybar (Roobol and Camp, 1991) match the archaeomagnetic direction at 641 C.E., shifting the understood vent site about 160 kilometers (km) north-northeast from its formerly interpreted location.

Lastly, it was anticipated that 5–10 percent of recovered mean remanent directions for the products of single eruptions would be found to be anomalous and exceed the range of ordinary geomagnetic secular variation (colatitude >22° N.) anticipated for this latitude. At least 13 lava flow and vent complexes defined by geologic mapping of Harrat Rahat (~6 percent) have measured mean remanent directions that are anomalous. Thus, the anomalous measurements indicate the lavas acquired their directions during brief geomagnetic cryptochrons during the Brunhes Normal Polarity Chron. These examples of geomagnetic excursions were erupted in the brief time spans (<2,000 years) of geomagnetic cryptochrons, when the Earth's magnetic field deviated from a simple axial dipole orientation and varied widely and rapidly. Oceanic sediments commonly record these cryptochrons, and their ages have been determined through ^{18}O/^{16}O dating methods (Oda, 2005). Geomagnetic cryptochrons identified in the remanent magnetization of ^{40}Ar/^{39}Ar dated volcanic rocks, combined with continuing study of oceanic sediments, were recently compiled by Channell and others (2020). Thus, identification of an anomalous remanent direction in a Harrat Rahat lava flow offers the opportunity to improve existing ^{40}Ar/^{39}Ar age assessments, guided by geologic mapping, stratigraphy, and geochemical correlations.

Methods

Paleomagnetic samples were collected, processed, and interpreted using conventional methods described by McElhinny (1973). An essential part of these methods is the sampling selection of a lava flow outcrop, noting the separate blocks that compose it, and establishing that they have not moved discernably after acquiring their remanent magnetization. This is a subjective judgment of the person taking the samples and only improves with experience. Samples were collected in the field with a handheld, gasoline-powered, 2.5-centimeter (cm) diameter coring drill and all were oriented using both sun and magnetic compasses. Generally, eight 10-cm-long cylindrical samples were collected at each site. Specimens that are 2.2 cm long were cut from the larger cylinders and measured using an automatic cryogenic magnetometer at the U.S. Geological Survey Menlo Park facility and subjected to progressive alternating-field (AF) demagnetization to remove secondary components of magnetization. An isothermal remanent magnetization (IRM) resulting in high magnetic sample intensities caused by proximal lightning strikes was the principal source of secondary magnetization. Care was taken during AF demagnetization to populate the lowest coercivity intervals of samples with multiple steps to establish the earliest part of the arc connecting the direction of the sample's fundamental IRM overprint to the direction of the original thermoremanent magnetization (TRM); two vectors in space define a great circle arc. This caution improves the precision of the intersection of separate sample arcs of the planes solution for a sample from sites (<5 percent) for which AF demagnetization cannot ultimately separate the IRM and TRM (Kirschvink, 1980).

The characteristic direction of remanent magnetization for each site was calculated using Fisher statistics on directional data from individual core demagnetization line fits using vector component diagrams, plane fits on equal-area diagrams, or mixtures of lines and planes data (Kirschvink, 1980). Results from each site are presented in table 1. We collected samples at a total of 178 sites: 173 within northern Harrat Rahat and 5 sites collectively within Harrat Khaybar and Harrat Ithnayn (figs. 1, 2).

Comparing the mean remanent magnetic directions of the youngest lava flows of Harrat Rahat and using calibrated archaeomagnetic records to assign eruption ages is a major contribution of this study. Assigning eruption ages using precise measurements of paleomagnetic directions requires reference to an independently dated paleomagnetic secular variation record for the area of interest. Archeological studies are commonly the best sources of such calibrations, but literature search failed to discover archaeomagnetic reference information with sufficient continuous age and geomagnetic control from areas close to Harrat Rahat. However, age-calibrated records are available from adjacent areas that are adequate to analyze the archaeomagnetic age of middle to late Holocene lava flows in our study area. Appropriate records come principally from Italy, Bulgaria, Turkey, Israel/Palestinian Territories, and Iran. Using the virtual geomagnetic pole (VGP) transformation (Gauss and Weber, 1838), archaeomagnetic control points from these adjacent regions can be recalculated to Harrat Rahat's location and then directly compared to the characteristic remanent directions we derive from the sampled lava flows.

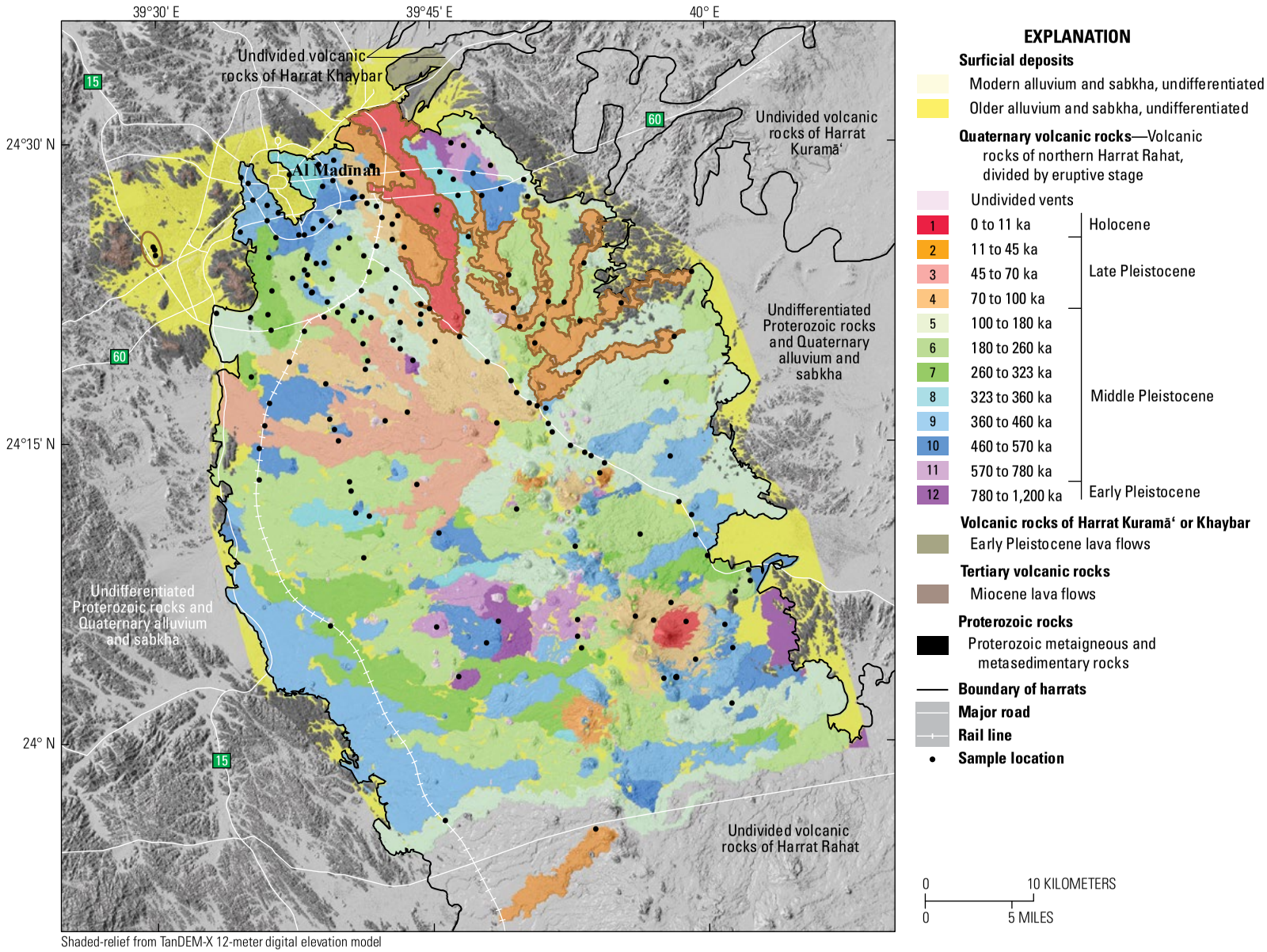

Figure 2. Geologic map of northern Harrat Rahat showing the locations of paleomagnetic core sampling. Flows outlined in brown are the basalt of Al Labah (1256 C.E; red), the Five Fingers lava flows (orange), and the small cinder cones and flows of the basalt of Al Du'aythah attributed in some prior studies to have erupted in 641 C.E. (ellipse west of Al Madīnah). Gray regions were not mapped as part of the recent Saudi Geological Survey and U.S. Geological Survey study. ka, kilo-annum, or thousands of years before present.

Table 1. Paleomagnetic results from sites in northern Harrat Rahat and additional sites in Harrats Khaybar and Ithnayn.

[Geologic unit names and labels from Downs and others (2019) and Robinson and Downs (2023). Mean values are shown in bold. Anomalous virtual geomagnetic pole (VGP) latitudes that are lower than 68° (colatitudes >22°) are shaded in yellow. –, not determined; ka, kilo-annum or thousand years before present]

Code[a]	Site ID[b]	Age[c] (ka)	Lat.[d] (°N)	Long.[d] (°E)	N/N$_o$[e]	Treatment[f]	Inclination[g]	Declination[h]	α95[j]	k[k]	R[l]	Pole lat. (°N)[m]	Pole long. (°E)[m]
Eruptive Stage 1 (0 to 11 ka)													
Basalt of Al Labah (unit bla), historical flow of 1256 C.E.													
R14DC033	8034B	0.8±0.2	24.3649	39.7480	8/8	Li	30.2	11.3	3.5	256	7.9727	76.7	165.2
R14DC034	8114B	–	24.3411	39.7759	8/8	Li	31.2	9.9	1.2	1,977	7.9965	78.1	166.9
R14DC049	9324B	–	24.4772	39.7243	8/8	Li	30.2	9.1	1.9	855	7.9918	78.1	172.1
Mean			**24.4**	**39.75**	**3/3**		**30.5**	**10.1**	**1.7**	**5,227**	**2.9996**	**77.6**	**168.0**
Trachyte of Um Rgaibah (unit trg)													
R17DC018	1367B	4.2±5.2	24.1017	39.9809	8/8	Li	27.5	8.4	3.6	240	7.9709	77.6	178.7
Eruptive Stage 2 (11 to 45 ka)													
Basalt of Al Du'aythah (unit bdu), cones and flows													
R15DC012	0895B	13.3±1.9	24.4148	39.4975	8/8	Li	51.0	12.9	3.2	307	7.9772	76.5	93.9
R15DC013	0975B	–	24.4173	39.4962	8/8	Mx	50.1	14.5	2.9	381	7.9816	75.6	99.5
R15DC014	1055B	–	24.4102	39.4987	8/8	Li	44.4	12.1	2.4	518	7.9865	78.9	118.2
Mean			**24.416**	**39.497**	**2/3**		**50.6**	**13.7**	**3.0**	**7,121**	**2.9999**	**76.1**	**96.9**
Basalt of Ad Duwaykhilah (unit bdw)													
R15DC037	2895B	25.6±16.2	24.4845	39.6960	8/9	Li	41.1	14.7	2.1	713	7.9902	76.6	130.7
R16DC018	1396B	–	24.4429	39.7199	7/8	Li	40.2	11.8	2.0	893	6.9933	79.1	135.4
R16DC021	1636B	–	24.4165	39.7256	7/8	Li	36.9	11.2	4.0	233	6.9742	79.0	147.9
Mean			**24.45**	**39.71**	**3/3**		**39.4**	**12.5**	**4.0**	**943**	**2.9979**	**78.3**	**137.6**
Basalt of Southern Fingers (unit bsof)													
R14DC001[n]	5434B	24.4±1.3	24.3111	39.8843	9/9	Li	45.5	5.6	1.1	2,172	8.9963	84.3	101.0
R14DC002[n]	5524B	–	24.3688	39.9239	7/9	Li	42.3	0.6	3.2	358	6.9833	89.5	116.5
R14DC003[n]	5614B	–	24.3949	39.9881	7/8	Li	44.3	9.3	1.5	1,627	6.9963	81.4	117.0
R14DC006[n]	5854B	–	24.3403	39.9717	8/8	Li	41.6	5.0	3.1	324	7.9784	85.4	113.6
Mean[n]		**24.6±1.2**	**24.35**	**39.94**	**4/4**		**43.5**	**5.1**	**3.6**	**660**	**3.9955**	**85.3**	**116.6**
Basalt of Northern Fingers (unit bnof)													
R14DC007[n]	5934B	22.0±3.3	24.3495	39.8304	7/8	Li	34.0	354.6	2.2	783	6.9923	82.4	262.1
R14DC008[n]	6014B	–	24.3703	39.8572	7/8	Mx	36.8	359.4	2.7	545	6.9890	86.1	228.2
R14DC009[n]	6094B	–	24.3650	39.8251	8/8	Li	34.4	354.8	1.6	1,147	7.9939	82.7	262.4
Mean[n]		**24.6±1.2**	**24.36**	**39.84**	**3/3**		**35.1**	**356.2**	**4.1**	**915**	**2.9978**	**83.9**	**255.5**
Basalt of Central Finger (unit bcef)													
R14DC004[n]	5694B	29±4	24.4024	39.8901	7/8	Li	38.4	0.1	2.4	661	6.9909	87.2	218.5
R14DC005[n]	5774B	–	24.3356	39.8440	8/8	Li	37.4	1.6	2.7	434	7.9839	86.3	196.5
Mean[n]		**24.6±1.2**	**24.37**	**39.87**	**2/2**		**37.9**	**0.9**	**3.4**	**5,472**	**1.9998**	**86.8**	**205.4**
Hawaiite of Khamisah (unit hkh)													
R14DC027	7554B	29.0±3.0	23.9289	39.8971	8/8	Li	68.7	335.4	3.1	327	7.9786	56.2	12.5
Eruptive Stage 3 (45 to 70 ka)													
Hawaiite of Al Anahi 3 (unit han3)													
R14DC011	6254B	51.0±9.0	24.2688	39.8098	7/8	Li	16.7	16.2	3.5	292	6.9794	67.9	172.6
R14DC042	8764B	–	24.3584	39.6519	8/8	Li	16.8	14.4	2.9	363	7.9807	69.1	176.2
Mean			**24.31**	**39.73**	**2/2**		**16.8**	**15.3**	**3.8**	**4,406**	**1.9998**	**68.5**	**174.3**

Table 1. Paleomagnetic results from sites in northern Harrat Rahat and additional sites in Harrats Khaybar and Ithnayn.—Continued

Code[a]	Site ID[b]	Age[c] (ka)	Lat.[d] (°N)	Long.[d] (°E)	N/N_o[e]	Treatment[f]	Inclination[g]	Declination[h]	α95[j]	k[k]	R[l]	Pole lat. (°N)[m]	Pole long. (°E)[m]
Eruptive Stage 3 (45 to 70 ka)—Continued													
Basalt of Musawda'ah (unit bms)													
R14DC012	6334B	59.1±5.7	24.1913	39.6925	7/9	Mx	33.4	3.7	2.7	592	6.9899	83.1	188.9
R14DC013	6424B	–	24.2178	39.7364	7/8	Li	37.2	7.5	3.9	242	6.9752	82.3	154.9
R14DC039	8524B	–	24.2545	39.6643	7/8	Mx	37.7	357.8	3.2	360	6.9834	86.3	253.1
R15DC044	3465B	–	24.2673	39.5976	8/8	Li	34.0	2.0	2.4	542	7.9871	84.1	200.7
R14DC010	6174B	–	24.2711	39.7075	8/8	Li	32.8	4.2	2.0	763	7.9908	82.5	187.3
Mean			**24.24**	**39.68**	**5/5**		**35.1**	**3.1**	**3.5**	**493**	**4.9919**	**84.3**	**189.0**
Eruptive Stage 4 (70 to 100 ka)													
Mugearite of Hill 1125 (unit mh11); separated into two flow groups													
R16DC035	2766B	–	24.3534	39.7216	6/8	Mx	34.4	358.7	7.7	89	5.9436	84.4	232.5
R16DC037	2926B	–	24.3375	39.7534	4/8	Mx	29.9	3.5	4.2	637	3.9953	81.1	197.5
Mean			**24.34**	**39.74**	**2/2**		**32.2**	**1.2**	**13.3**	**357**	**1.9972**	**83.0**	**210.6**
R15DC028[n]	2175B	–	24.2829	39.8461	8/8	Mx	22.1	355.4	2.6	477	7.9853	76.5	239.5
R15DC030[n]	2335B	–	24.2942	39.8275	8/8	Mx	23.9	358.0	3.1	344	7.9797	78.1	229.3
Mean[n]			**24.28**	**39.83**	**2/2**		**23.0**	**356.7**	**6.5**	**1,464**	**1.9993**	**77.3**	**234.7**
Basalt of Sha'ib Al Khakh (unit bsk)													
R14DC038[n]	8434B	–	24.3023	39.6538	5/9	Mx	21.9	346.6	3.3	629	4.9936	71.9	266.5
R15DC042[n]	3305B	–	24.3209	39.6203	7/8	Li	21.4	356.8	2.1	849	6.9929	76.5	233.0
R16DC046[n]	3646B	–	24.2727	39.6570	8/8	Mx	26.6	355.4	2.1	700	7.9900	78.9	243.5
R17DC014[n]	1077B	–	24.2784	39.7275	5/8	Pl	22.5	0.7	29.7	4	–	77.4	216.6
Mean[n]			**24.30**	**39.64**	**3/4**		**23.4**	**352.9**	**8.9**	**192**	**2.9896**	**76.2**	**249.9**
Trachyte of Gura 5 (unit tg5)													
R17DC019[n]	1447B	79.7±1.6	24.1033	39.9514	8/8	Li	50.4	339.4	3.0	345	7.9797	70.5	335.7
Trachyte of Gura 4 (unit tg4)													
R17DC020[n]	1527B	84.3±1.6	24.1066	39.9343	8/8	Mx	51.3	346.3	3.2	306	7.9771	75.6	346.1
Trachyte of Al Efairia (unit tef)													
R17DC017	1287B	88.0±1.8	24.0703	39.9888	8/8	Mx	37.8	4.3	2.6	477	7.9853	85.1	165.0
Basalt of As Suddiyah (unit bsu)													
R15JR006	0415A	85.7±5.7	24.4712	39.6767	6/8	Mx	42.3	351.4	8.8	61	5.9183	82.2	311.4
R15DC024	1855B	–	24.4532	39.6920	8/8	Li	41.4	354.1	1.6	1,268	7.9945	84.5	304.0
R15DC036	2815B	–	24.4413	39.7058	8/8	Li	36.8	356.4	2.4	542	7.9871	84.8	260.8
R16DC005	0346B	–	24.4587	39.6873	8/8	Mx	42.7	355.6	2.4	557	7.9874	86.0	315.0
R16DC019	1476B	–	24.4356	39.7148	7/8	Li	40.5	355.5	2.9	428	6.9860	85.7	293.0
R16DC020	1556B	–	24.4230	39.7146	8/8	Mx	39.5	354.5	2.1	721	7.9903	84.6	289.0
Mean			**24.45**	**39.70**	**6/6**		**40.5**	**354.6**	**2.1**	**1,011**	**5.9951**	**84.9**	**296.1**
Eruptive Stage 5 (100 to 180 ka)													
Basalt of Umm Nathilah (unit bun)													
R16DC001	0016B	105.0±8.6	24.3579	39.5852	6/8	Mx	58.5	349.9	3.0	553	5.9910	72.9	12.1
R16DC002	0096B	–	24.3617	39.5539	8/8	Li	57.5	346.2	2.4	516	7.9864	71.9	2.5
Mean			**24.36**	**39.57**	**2/2**		**58.0**	**348.0**	**4.8**	**2,711**	**1.9996**	**72.5**	**7.1**

Table 1. Paleomagnetic results from sites in northern Harrat Rahat and additional sites in Harrats Khaybar and Ithnayn.—Continued

Code[a]	Site ID[b]	Age[c] (ka)	Lat.[d] (°N)	Long.[d] (°E)	N/N$_o$[e]	Treatment[f]	Inclination[g]	Declination[h]	α95[i]	k[k]	R[l]	Pole lat. (°N)[m]	Pole long. (°E)[m]
Eruptive Stage 5 (100 to 180 ka)—Continued													
Mugearite of Mukhayar (unit mmk)													
R14DC030	7794B	114.4±8.5	24.0332	40.0224	7/8	Li	41.3	12.0	3.9	238	6.9748	79.0	129.3
Basalt of Shai'ab Abu Sikhbir (unit bsas)													
R15DC021[n]	1615B	115.3±7.5	24.2021	39.9749	8/8	Mx	34.7	358.9	3.3	293	7.9761	84.8	231.5
Mugearite of Dabaa 1 (unit md1)													
R14DC015[n]	6584B	116.7±2.8	24.2266	39.9029	8/8	Li	33.9	2.0	3.7	226	7.9690	84.1	200.9
Mean of units bsas and md1[n]			**24.21**	**39.94**	**2/2**		**34.3**	**0.5**	**5.9**	**1,824**	**1.9995**	**84.6**	**215.3**
Basalt of Abu Rimthah (unit bar)													
R15DC025	1935B	130.3±5.0	24.2439	39.8892	8/8	Mx	52.6	0.3	3.2	316	7.9778	81.1	41.5
Basalt of Nubala (unit bnu)													
R14DC043	8844B	131.2±8.3	24.3675	39.6689	6/8	Mx	33.5	357.7	3.5	371	5.9865	83.6	239.6
R14DC044	8924B	–	24.3801	39.6862	8/8	Mx	39.0	352.1	3.3	302	7.9768	82.4	293.4
R16DC028	2206B	–	24.3623	39.6859	8/8	Mx	31.9	359.2	2.3	598	7.9883	82.9	225.9
Mean			**24.37**	**39.68**	**3/3**		**34.8**	**356.5**	**7.3**	**285**	**2.9930**	**83.9**	**252.8**
Basalt of Nashbah (unit bns)													
R14DC026	7474B	134.1±24.3	23.9366	39.7603	8/8	Mx	37.1	24.0	3.3	337	7.9792	67.6	133.3
Basalt of Mahd Adh Thahab Road (unit bmat)													
R15DC033	2575B	136.7±7.6	24.3977	39.7094	8/8	Li	44.0	354.1	2.1	693	7.9899	84.5	325.4
R15DC035	2735B	–	24.4175	39.7002	7/8	Li	45.7	359.8	3.3	334	6.9821	87.3	35.9
R16DC038	3006B	–	24.3605	39.7407	8/8	Mx	41.2	351.4	3.2	329	7.9787	82.1	306.3
R16DC040	3166B	–	24.3685	39.7403	8/8	Li	45.7	358.1	2.4	544	7.9871	86.8	8.2
Mean			**24.39**	**39.72**	**4/4**		**44.2**	**355.8**	**3.9**	**545**	**3.9945**	**85.9**	**332.4**
Basalt of Sha'ib Banthane (unit bsb)													
R16DC032	2526B	–	24.3314	39.7215	8/8	Mx	30.9	349.3	3.6	275	7.9746	77.4	274.3
Basalt of Al Muzayyin (unit bmz)													
R16DC031	2446B	–	24.3387	39.7154	8/8	Mx	46.9	9.7	3.3	288	7.9757	80.5	104.2
R16DC033	2606B	–	24.3822	39.7174	8/8	Mx	46.8	9.1	3.0	362	7.9806	81.1	103.7
Mean			**24.36**	**39.716**	**2/2**		**46.9**	**9.4**	**0.9**	**73,584**	**1.9999**	**80.8**	**103.9**
Hawaiite of Al Anahi 1 (unit han1)													
R15DC052	4105B	139.0±5.4	24.4092	39.6890	7/8	Li	50.2	341.6	1.8	1,184	6.9949	72.4	335.6
Basalt of Al Rafi'ah (unit bra)													
R15JR007	0495A	–	24.4462	39.6660	7/8	Mx	44.9	356.5	2.9	386	7.9818	86.2	343.2
R16DC008	0586B	–	24.4507	39.7007	7/8	Li	46.4	353.7	5.7	114	6.9473	83.5	341.0
R16DC034	2686B	–	24.3713	39.7133	8/8	Mx	37.2	359.2	2.4	653	7.9893	86.3	231.5
Mean			**24.42**	**39.69**	**3/3**		**42.9**	**356.6**	**8.1**	**231**	**2.9913**	**86.9**	**319.0**
Basalt west of Abu Rimthah (unit bwar)													
R15DC026	2015B	–	24.2499	39.8767	8/8	Li	37.9	6.9	3.6	233	7.9699	83.0	156.3
Basalt of Hill 1066 (unit bh10)													
R15DC029[n]	2255B	137.3±11.3	24.2854	39.8389	8/8	Mx	31.3	359.6	1.4	1,676	7.9958	82.6	222.8

Table 1. Paleomagnetic results from sites in northern Harrat Rahat and additional sites in Harrats Khaybar and Ithnayn.—Continued

Code[a]	Site ID[b]	Age[c] (ka)	Lat.[d] (°N)	Long.[d] (°E)	N/N$_o$[e]	Treatment[f]	Inclination[g]	Declination[h]	α95[j]	k[k]	R[l]	Pole lat. (°N)[m]	Pole long. (°E)[m]
Eruptive Stage 5 (100 to 180 ka)—Continued													
Basalt of Sha'ib Iskabah (unit bsi)													
R14DC037[n]	8354B	151.9±9.9	24.2613	39.8599	7/8	Li	31.5	0.0	3.4	320	6.9813	82.8	220.9
R15DC027[n]	2095B	–	24.2684	39.8559	8/8	Li	31.2	359.0	1.7	1,065	7.9934	82.5	227.2
Mean[n]			**24.26**	**39.86**	**2/2**		**31.4**	**359.5**	**2.0**	**16,009**	**1.9999**	**82.7**	**223.6**
Basalt of Ad Dubaysiyah (unit bdy)													
R14DC035	8194B	139.2±11.3	24.3203	39.8005	8/8	Li	25.9	8.2	2.6	454	7.9846	76.8	182.4
R16DC041	3246B	–	24.3621	39.7827	8/8	Mx	26.1	6.9	3.6	301	7.9768	77.6	187.0
Mean			**24.34**	**39.79**	**2/2**		**26.0**	**7.6**	**2.6**	**9,352**	**1.9999**	**77.2**	**184.6**
Basalt of Nabta (unit bna)													
R14DC047	9164B	162.9±11.1	24.4846	39.8049	8/8	Mx	52.8	358.3	2.1	740	7.9905	81.0	30.7
R15DC038	2985B	–	24.4726	39.8355	8/8	Mx	49.1	357.5	2.0	822	7.9915	84.1	18.5
R16DC051	4046B	–	24.4585	39.8390	8/8	Li	48.1	356.9	1.8	960	7.9927	84.6	9.4
Mean			**24.47**	**39.83**	**3/3**		**50.0**	**357.5**	**3.8**	**1,037**	**2.9981**	**83.3**	**21.4**
Basalt of Al Khanaq (unit bka)													
R14DC046[n]	9084B	144.6±19.6	24.5125	39.7943	8/8	Mx	41.7	344.5	3.9	217	7.9678	75.9	311.0
Basalt of Ash Suqayyiqah (unit bsq)													
R16DC043[n]	3406B	–	24.3144	39.6899	8/8	Mx	44.1	352.2	4.9	148	7.9528	82.8	323.6
Eruptive Stage 6 (180 to 260 ka)													
Basalt of Ar Rummanah (unit bru)													
R15DC034[n]	2655B	–	24.3959	39.6937	8/8	Mx	46.7	329.2	3.6	270	7.9741	62.2	323.8
R16DC012[n]	0906B	–	24.4243	39.6760	6/8	Mx	49.0	336.3	4.2	324	5.9846	68.3	329.5
R16DC015[n]	1146B	–	24.4161	39.6652	8/9	Mx	43.0	331.9	2.0	1,004	7.9930	64.5	316.9
Mean[n]			**24.41**	**39.68**	**3/3**		**46.3**	**332.4**	**5.9**	**435**	**2.9954**	**65.0**	**323.0**
Basalt of Al Jassah (unit bjs)													
R14DC041[n]	8684B	–	24.3464	39.6341	8/8	Mx	48.5	331.8	3.3	318	7.9780	64.4	327.4
Basalt of Shuran (unit bsh)													
R15DC008[n]	0575B	191.5±4.2	24.3908	39.6238	8/8	Mx	22.4	26.4	2.0	880	7.9920	61.9	151.9
R15DC031[n]	2415B	–	24.3976	39.6345	7/8	Li	22.7	26.1	3.2	349	6.9828	62.3	151.9
R16DC027[n]	2116B	–	24.3622	39.6642	9/9	Mx	28.9	19.4	4.8	125	8.9362	69.7	152.2
R16DC030[n]	2366B	–	24.3359	39.6877	6/8	Mx	28.7	31.5	10.7	56	5.9104	59.1	140.8
R16DC029[n]	2286B	–	24.3574	39.6948	7/8	Li	17.9	22.7	2.8	468	6.9872	63.6	160.9
Mean[n]			**24.37**	**39.66**	**5/5**		**24.2**	**25.2**	**5.9**	**171**	**4.9767**	**63.5**	**151.3**
Basalt of Shuran vent (unit bsh)													
R16DC044[n]	3486B		24.3216	39.6919	7/8	Mx	45.6	4.7	2.3	824	6.9927	85.0	95.9
Mugearite of Um Zhabah 2 (unit mz2)													
R15DC017[n]	1295B	195.9±1.3	24.1447	40.0382	6/8	Mx	25.2	37.5	5.4	193	5.9741	53.0	140.3
R16DC053[n]	4206B	–	24.0802	39.8853	6/8	Mx	39.2	22.5	11.0	44	5.8857	69.2	130.6
R14DC032[n]	7954B	–	24.1270	40.0253	7/8	Mx	44.7	4.3	5.6	121	6.9503	85.5	99.6
R16DC055[n]	4366B	–	24.1356	40.0394	7/8	Li	47.3	355.1	4.6	175	6.9657	83.9	355.2
R16DC054[n]	4286B	–	24.1177	39.9675	5/8	Mx	43.6	9.6	4.7	418	4.9904	81.2	119.2
R16DC052[n]	4126B	–	24.1038	39.8818	5/8	Mx	49.8	359.3	5.1	236	4.9831	83.5	34.6
Mean[n]			**24.12**	**40.0**	**4/6**		**46.5**	**2.3**	**5.9**	**248**	**3.9879**	**85.8**	**68.9**

Table 1. Paleomagnetic results from sites in northern Harrat Rahat and additional sites in Harrats Khaybar and Ithnayn.—Continued

Code[a]	Site ID[b]	Age[c] (ka)	Lat.[d] (°N)	Long.[d] (°E)	N/N$_o$[e]	Treatment[f]	Inclination[g]	Declination[h]	α95[j]	k[k]	R[l]	Pole lat. (°N)[m]	Pole long. (°E)[m]
Eruptive Stage 6 (180 to 260 ka)—Continued													
Basalt of Lower Qa Al Aqul (unit blqa)													
R14DC045	9004B	196.9±10.3	24.5170	39.7976	7/8	Li	31.1	359.1	3.5	300	6.9800	82.2	226.2
Basalt of Qa Al Ghusun (unit bqg)													
R14DC040[n]	8604B	–	24.2203	39.6746	8/8	Mx	40.7	18.0	3.3	296	7.9764	73.5	129.3
R15DC048[n]	3785B	215.2±6.9	24.2126	39.6762	8/8	Mx	46.0	8.0	4.1	193	7.9638	82.1	104.3
Mean[n]			**24.22**	**39.675**	**2/2**		**43.5**	**13.2**	**19.7**	**163**	**1.9939**	**78.0**	**121.5**
Basalt of Abu Ghuwayshiyah (unit bag)													
R17DC001[n]	0017B	220.3±8.3	24.3516	39.8519	7/8	Mx	40.9	19.4	2.9	431	6.9861	72.3	128.9
R17DC002[n]	0097B	–	24.3699	39.8719	8/8	Mx	40.7	19.8	6.7	80	7.9119	71.9	129.3
R17DC003[n]	0187B	–	24.3538	39.8858	6/8	Mx	41.5	23.2	2.4	858	5.9942	68.8	126.4
Mean[n]			**24.36**	**39.87**	**3/3**		**41.1**	**20.8**	**2.5**	**2,483**	**2.9992**	**71.0**	**128.1**
Hawaiite of Al Malsa (unit hma)													
R14DC017	6744B	220.5±10.9	24.3927	39.8210	7/8	Li	15.9	356.1	4.5	185	6.9676	73.3	233.5
Mugearite of Al Mulaysa (unit mmu)													
R14DC019	6904B	219.6±4.0	24.1654	39.8801	7/8	Mx	37.6	2.9	3.0	497	6.9879	85.9	178.6
Basalt of Umm Sufar (unit bsf)													
R15DC050	3945B	217.5±6.7	24.1567	39.6877	8/8	Li	59.7	349.8	3.7	223	7.9687	71.5	14.6
Basalt of Banthane Dam (unit bbd)													
R16DC014[n]	1066B	223.4±8.6	24.4075	39.6365	7/8	Mx	26.5	357.7	3.7	322	6.9814	79.4	231.8
R16DC016[n]	1236B	–	24.3902	39.6599	7/8	Mx	25.8	9.1	3.2	423	6.9858	76.2	179.5
R16DC017[n]	1316B	–	24.3935	39.6370	5/8	Mx	27.8	10.1	2.8	768	4.9948	76.5	173.2
Mean[n]			**24.392**	**39.64**	**2/3**		**26.8**	**9.6**	**4.8**	**2,738**	**2.9996**	**76.4**	**176.4**
Basalt of Lower Sha'ib Lihyan (unit blsl)													
R17DC022[n]	1687B	228.6±12.0	24.3026	39.9641	8/8	Mx	30.5	7.7	4.2	194	7.9639	79.3	176.1
Basalt of Sha'ib Hayaya (unit bhy)													
R14DC016[n]	6664B	235.1±7.5	24.1752	39.9393	8/8	Li	29.5	357.3	3.5	256	7.9727	81.3	237.0
Basalt of Abu Siyilah (unit bsy)													
R15DC046[n]	3625B	236.2±29.2	24.2221	39.5921	4/8	Mx	29.7	355.7	5.2	347	3.9913	80.8	246.3
Benmoreite of Al Bayadah (unit oba)													
R14DC018	6824B	242.8±2.4	24.1968	39.8273	6/8	Pl	47.8	43.8	2.2	675	7.1584	50.8	113.2
Basalt of Al Billa'ah (unit bli)													
R14DC036	8274B	–	24.3043	39.8223	8/8	Mx	42.4	330.6	4.5	183	7.9618	63.3	316.5
Eruptive Stage 7 (260 to 323 ka)													
Hawaiite of As Sabah (unit hsb)													
R15DC020	1535B	271.6±62.9	24.1914	39.9865	7/8	Mx	55.6	118.1	5.3	173	6.9653	−6.1	85.7
Basalt of Al Huzaym (unit bhu)													
R15DC007[n]	0495B	285.1±6.6	24.4080	39.6021	8/8	Mx	44.8	18.6	1.9	943	7.9926	73.1	118.9
R15DC009[n]	0655B	–	24.3476	39.6039	8/8	Li	44.7	25.0	3.3	281	7.9751	67.4	119.3
R15DC010[n]	0735B	–	24.3604	39.6009	8/8	Li	45.9	25.7	2.8	391	7.9821	66.8	116.8
R15DC011[n]	0815B	–	24.3802	39.6048	7/8	Li	44.0	24.9	2.0	927	6.9935	67.4	120.8
R15DC015[n]	1135B	–	24.4249	39.6086	8/8	Mx	43.3	26.0	3.2	314	7.9777	66.4	122.2
Mean[n]			**24.38**	**39.604**	**5/5**		**44.6**	**24.1**	**2.3**	**1,146**	**4.9965**	**68.2**	**119.6**

Table 1. Paleomagnetic results from sites in northern Harrat Rahat and additional sites in Harrats Khaybar and Ithnayn.—Continued

Code[a]	Site ID[b]	Age[c] (ka)	Lat.[d] (°N)	Long.[d] (°E)	N/N$_o$[e]	Treatment[f]	Inclination[g]	Declination[h]	α95[i]	k[k]	R[l]	Pole lat. (°N)[m]	Pole long. (°E)[m]
Eruptive Stage 7 (260 to 323 ka)—Continued													
Basalt of An Nughayr (unit bau)													
R16DC042[n]	3326B	–	24.3086	39.5854	6/8	Pl	47.0	23.2	5.3	116	–	68.9	113.9
Basalt of Hill 865 (unit bh86)													
R15DC047	3705B	285.4±20.1	24.0998	39.6571	8/8	Li	32.0	344.6	2.0	758	7.9908	74.1	287.5
Basalt of Dabaa 3 (unit bd3)													
R15DC018	1375B	307.7±4.6	24.1569	40.0008	8/8	Mx	47.0	5.4	3.6	258	7.9729	83.7	89.0
Eruptive Stage 8 (323 to 360 ka)													
Basalt of Al Mustarah (unit bmu)													
R15JR004	0255A	344.7±4.8	24.4774	39.6212	8/8	Mx	47.9	350.6	1.2	2,272	7.9969	80.5	339.8
R15JR005	0335A	–	24.4675	39.6516	7/8	Mx	46.3	357.1	4.9	164	6.9633	85.9	0.7
R16DC039	3086B	–	24.3522	39.7398	8/8	Mx	48.6	347.1	2.7	432	7.9838	77.4	336.9
Mean			**24.43**	**39.67**	**3/3**		**47.7**	**351.7**	**5.5**	**499**	**2.9960**	**81.4**	**341.7**
Basalt of Lower Sahab (unit blsa)													
R15DC041	3225B	346.9±9.9	24.4595	39.7750	8/8	Li	41.7	18.4	2.0	779	7.9910	73.2	127.5
R16DC047	3726B	–	24.4793	39.7582	8/8	Mx	31.7	10.8	3.8	255	7.9726	77.5	163.7
R16DC048	3806B	–	24.4731	39.7705	5/8	Mx	21.6	49.8	5.1	237	4.9831	41.1	136.3
R17DC015	1157B	–	24.4251	39.7838	8/8	Pl	46.5	347.3	5.1	94	–	78.1	328.9
Eruptive Stage 9 (360 to 460 ka)													
Basalt of Upper Abu Rimthah (unit burr)													
R15DC022	1695B	366.4±9.3	24.2349	39.9073	8/8	Mx	41.0	3.8	4.4	182	7.9615	86.5	141.2
R15DC023	1775B	–	24.2411	39.8948	7/8	Li	39.5	3.1	3.1	1,344	6.9955	86.6	162.2
R17DC021	1607B	–	24.2404	39.9676	8/8	Li	40.9	354.9	2.2	625	7.9888	85.3	301.0
Mean			**24.24**	**39.92**	**3/3**		**40.5**	**0.6**	**5.9**	**444**	**2.9955**	**88.8**	**192.3**
Basalt of Powerline Road (unit bpr)													
R16DC050[n]	3966B	378.8±10.0	24.4471	39.7556	8/8	Li	53.7	353.5	1.7	1,102	7.9937	78.7	11.2
Basalt of Al Harrah Al Gharbiyah (unit bhg)													
R15DC001[n]	0015B	382.5±5.8	24.4703	39.5831	8/8	Mx	44.7	352.3	2.6	540	7.9870	82.8	326.2
R15DC002[n]	0095B	–	24.4753	39.5767	8/8	Li	54.7	342.3	1.2	2,303	7.9970	71.3	348.6
R15DC003[n]	0175B	–	24.4391	39.6007	7/8	Mx	55.3	352.0	1.9	1,105	6.9946	76.7	10.3
R15DC004[n]	0255B	–	24.4519	39.6006	8/8	Mx	54.8	343.5	2.4	558	7.9874	72.1	350.8
R15DC005[n]	0335B	–	24.4454	39.6106	8/8	Mx	53.3	348.2	2.3	583	7.9880	76.1	354.8
R15DC006[n]	0415B	–	24.4565	39.5877	8/8	Mx	58.0	346.7	3.2	322	7.9782	71.9	4.3
R15DC051[n]	4025B	–	24.4296	39.5760	7/8	Li	56.2	349.7	1.4	1,936	6.9969	74.8	6.4
Mean[n]			**24.45**	**39.59**	**6/7**		**55.4**	**347.1**	**2.2**	**943**	**5.9947**	**74.0**	**358.5**
Mugearite of Umm Qurah (unit muq)													
R15DC019	1455B	385.6±12.6	24.1744	39.9899	8/8	Li	39.9	25.6	3.2	311	7.9775	66.6	128.4
Basalt of Quraydah (unit bqr)													
R15DC032	2495B	380.7±165.9	24.4037	39.6526	7/8	Li	44.3	356.8	2.0	945	6.9937	86.7	338.8
R16DC011	0826B	–	24.4387	39.6508	7/8	Mx	46.4	352.7	3.0	405	6.9852	82.7	337.7
R16DC010	0746B	–	24.4323	39.6424	6/8	Mx	68.5	50.4	9.6	70	5.9284	43.2	80.5
R16DC013	0986B	–	24.4029	39.6450	7/8	Mx	84.3	60.4	13.1	25	6.7612	29.6	50.9
Mean			**24.42**	**39.651**	**2/4**		**45.4**	**354.8**	**7.8**	**1,033**	**1.9990**	**84.7**	**338.2**

Table 1. Paleomagnetic results from sites in northern Harrat Rahat and additional sites in Harrats Khaybar and Ithnayn.—Continued

Code[a]	Site ID[b]	Age[c] (ka)	Lat.[d] (°N)	Long.[d] (°E)	N/N$_o$[e]	Treatment[f]	Inclination[g]	Declination[h]	α95[j]	k[k]	R[l]	Pole lat. (°N)[m]	Pole long. (°E)[m]
Eruptive Stage 9 (360 to 460 ka)—Continued													
Basalt of Al Urayd (unit bur)													
R15JR001	0015A	401.8±6.3	24.4859	39.6476	8/8	Mx	36.0	352.1	1.9	855	7.9918	81.4	279.5
R15JR002	0095A	–	24.4725	39.6610	8/8	Mx	37.2	356.4	2.5	511	7.9863	85.0	262.4
R15JR003	0175A	–	24.4896	39.6616	8/8	Pl	41.3	351.7	16.0	10	–	82.4	305.5
Mean			**24.48**	**39.66**	**3/3**		**38.2**	**353.4**	**5.3**	**550**	**2.9964**	**83.2**	**284.5**
Mugearite of Um Znabah 3 (unit mz3)													
R14DC031[n]	7874B	–	24.0991	40.0161	7/8	Mx	51.9	19.8	2.3	732	6.9918	70.7	99.7
Mugearite of Um Znabah 6 (unit mz6)													
R14DC024[n]	7314B	–	24.0550	39.9716	6/8	Li	53.8	18.2	3.2	446	5.9888	71.1	92.7
Trachyte of Um Znabah 6 (unit tz6)													
R14DC021[n]	7064B	–	24.0544	39.9604	9/9	Li	49.3	16.2	2.8	342	8.9766	74.4	103.3
Mean of units mz3, mz6, and tz6[n]			**24.07**	**39.98**	**3/3**		**51.7**	**18.0**	**3.9**	**1,028**	**2.9981**	**72.1**	**98.5**
Basalt north of Iskabah (unit bni)													
R14DC014	6504B	402.5±15.4	24.2813	39.8542	8/8	Mx	26.1	14.1	4.2	198	7.9647	73.0	165.6
Benmoreite of As Zayinah (unit ozy)													
R14DC022[n]	7154B	418.8±1.9	24.0556	39.9716	8/8	Li	8.8	351.2	2.7	429	7.9837	68.7	244.6
Basalt of Rahat (unit brh)													
R16DC022[n]	1716B	411.5±5.9	24.3709	39.6553	7/8	Mx	−13.8	56.7	5.9	123	6.9511	26.5	151.7
R16DC025[n]	1956B	–	24.3846	39.6358	8/8	Mx	1.1	351.4	2.9	393	7.9822	64.8	240.2
Benmoreite of Um Znabah 5 (unit oz5)													
R14DC023	7234B	449.6±6.6	24.0554	39.9713	7/8	Th	51.7	1.9	3.3	354	6.9831	81.6	51.0
Eruptive Stage 10 (460 to 570 ka)													
Basalt of Al Iskan (unit bis)													
R16DC007	0506B	467.7±78.8	24.4576	39.6787	8/8	Mx	43.9	351.9	2.3	619	7.9887	82.6	321.0
Basalt of Al Khafaq (unit bkf)													
R15DC043	3385B	>83	24.2864	39.6021	6/8	Mx	41.7	22.2	2.8	694	5.9928	69.8	125.8
R16DC045	3566B	–	24.2640	39.6616	7/8	Pl	38.8	30.9	3.6	216	–	61.5	128.1
Mean			**24.27**	**39.63**	**2/2**		**40.3**	**26.6**	**15.9**	**251**	**1.9960**	**65.6**	**127.1**
Basalt of Quba (unit bqu)													
R15DC016	1215B	476.1±70.5	24.4271	39.6293	8/8	Mx	55.6	17.6	1.4	1,640	7.9957	70.9	87.8
R16DC023	1796B	–	24.3786	39.6411	8/8	Mx	55.9	12.3	4.4	180	7.9612	74.0	78.0
Mean			**24.40**	**39.635**	**2/2**		**55.8**	**15.0**	**6.5**	**1,462**	**1.9993**	**72.5**	**83.3**
Basalt of Hathm (unit bha)													
R16DC006	0426B	476.1±70.5	24.4585	39.6805	7/8	Mx	61.5	5.9	2.0	1,067	6.9944	71.2	53.2
Basalt of Az Zinitah (unit bzi)													
R15DC045	3545B	>236	24.2484	39.5925	7/8	Li	43.2	10.3	2.6	538	6.9889	80.6	122.0
Basalt of Hill 838 (unit bh83)													
R15DC049	3865B	505.1±10.3	24.1943	39.6800	8/8	Mx	35.7	20.0	3.3	325	7.9785	71.4	139.6
Basalt of Hill 821 (unit bh82)													
R14DC048	9244B	507.4±38.3	24.4780	39.7891	8/8	Li	37.2	2.2	2.4	523	7.9866	85.8	190.8
R15DC039	3065B	–	24.4645	39.8140	8/8	Mx	39.4	4.5	2.3	673	7.9896	85.4	156.3
R15DC040	3145B	–	24.4595	39.7969	8/8	Mx	37.5	5.9	2.6	503	7.9861	83.6	161.1

Table 1. Paleomagnetic results from sites in northern Harrat Rahat and additional sites in Harrats Khaybar and Ithnayn.—Continued

Code[a]	Site ID[b]	Age[c] (ka)	Lat.[d] (°N)	Long.[d] (°E)	N/N_o[e]	Treatment[f]	Inclination[g]	Declination[h]	α95[j]	k[k]	R[l]	Pole lat. (°N)[m]	Pole long. (°E)[m]
Eruptive Stage 10 (460 to 570 ka)—Continued													
Basalt of Hill 821 (unit bh82)—Continued													
Mean			**24.47**	**39.8**	**3/3**		**38.0**	**4.2**	**2.9**	**1,819**	**2.9989**	**85.1**	**167.7**
Basalt of Upper Sha'ib Huquf (unit buph)													
R17DC004[n]	0267B	510.8±29.4	24.0851	39.7989	6/8	Li	−19.6	17.2	2.3	864	5.9942	51.9	191.6
Basalt of Al Farash (unit bfa)													
R17DC008[n]	0587B	–	24.1770	39.7557	7/8	Mx	−20.8	5.7	5.1	162	6.9630	54.6	210.1
Basalt of Al Ihn (unit bai)													
R16DC026[n]	2036B	546.2±9.6	24.3551	39.6794	8/8	Mx	43.4	350.8	1.6	1,271	7.9945	81.6	318.1
R16DC009[n]	0666B	–	24.4269	39.6343	8/8	Mx	39.8	349.3	1.5	1,350	7.9948	80.0	301.4
R16DC024[n]	1876B	–	24.3792	39.6416	6/8	Mx	39.7	352.2	6.6	118	5.9577	82.6	296.8
Mean[n]			**24.39**	**39.65**	**3/3**		**41.0**	**350.8**	**3.6**	**1,159**	**2.9983**	**81.5**	**305.3**
Basalt of Um Rgaibah (unit brg)													
R14DC025[n]	7394B	543.3±5.6	24.0797	40.0230	7/8	Mx	43.8	349.1	2.6	550	6.9891	80.0	321.1
Eruptive Stage 11 (570 to 780 ka)													
Basalt of Sha'ib Ad Dirwah (unit bsd)													
R14DC020	6984B	584.5±10.4	24.0900	39.8818	6/8	Mx	−12.3	23.1	3.4	445	5.9888	52.2	180.3
Basalt of Sha'ib Luwa (unit bsl)													
R16DC049	3886B	>507	24.5011	39.7800	7/8	Pl	42.5	355.5	3.3	257	–	85.9	312.3
Basalt of Al Jar'ah (unit bja)													
R17DC007	0507B	698.1±16.0	24.0986	39.7532	8/8	Mx	55.6	350.7	3.2	323	7.9783	75.5	8.3
Eruptive Stage 12 (780 to 1,200 ka)													
Basalt of Ghadwar (unit bgh)													
R17DC005	0347B	930.2±20.1	24.1030	39.8101	6/8	Mx	−45.4	181.2	2.0	1,373	5.9964	−87.0	240.8
R17DC006	0427B	–	24.0567	39.7734	8/8	Mx	−38.6	182.4	2.6	484	7.9855	−86.8	355.4
Mean			**24.08**	**39.79**	**2/2**		**−42.0**	**181.8**	**15.0**	**279**	**1.9964**	**−88.3**	**304.0**
Basalt of Hill 892 (unit bh89)													
R16DC036	2846B	1,014.0±14.0	24.3216	39.7331	8/8	Mx	−57.1	217.1	6.4	85	7.9178	−55.8	277.8
Basalt of Upper Qa Al Aqul (unit buqa)													
R17DC016	1237B	1,069.6±19.3	24.5034	39.7689	5/5	Pl	−32.6	192.3	3.9	258	–	−76.7	338.0
Other Unnamed Units													
Basalt south of Al Madīnah city center (unit v)													
R16DC003	0176B	>780	24.4097	39.6373	6/8	Mx	−35.0	176.6	7.7	107	5.9534	−84.0	72.0

Table 1. Paleomagnetic results from sites in northern Harrat Rahat and additional sites in Harrats Khaybar and Ithnayn.—Continued

Code[a]	Site ID[b]	Age[c] (ka)	Lat.[d] (°N)	Long.[d] (°E)	N/N_o[e]	Treatment[f]	Inclination[g]	Declination[h]	α95[j]	k[k]	R[l]	Pole lat. (°N)[m]	Pole long. (°E)[m]
Other Unnamed Units—Continued													
Unnamed basaltic vent southeast of Al Madīnah (unit v)													
R16DC004	0256B	>460	24.4344	39.6584	9/9	Mx	45.9	2.0	3.6	234	8.9658	86.6	71.4
Basalt on South Boundary Road (outside of map area)													
R14DC028	7634B	–	23.9477	39.9910	7/8	Mx	35.3	4.7	3.3	344	6.9825	83.8	174.4
R14DC029	7714B	–	23.9561	40.0466	8/8	Mx	37.8	8.4	3.9	244	7.9713	81.8	148.0
Mean			**23.95**	**40.02**	**2/2**		**36.6**	**6.5**	**8.5**	**871**	**1.9989**	**83.0**	**159.6**
Young Basalts of Harrat Khaybar and Harrat Ithnayn (Roobol and Camp, 1991)													
Basalt of Jabal Qidr													
R17DC009	0667B	1.8±0.4	25.7096	39.8002	8/8	Mx	39.6	0.1	2.0	789	7.9911	86.8	218.2
Basalt of Habir flow													
R17DC010	0747B	1.8±0.3	25.7949	39.8855	8/8	Li	45.1	3.4	1.4	1,545	7.9955	86.8	113.6
R17DC011	0827B	2.7±0.6	25.7798	39.9272	7/8	Li	40.4	3.0	1.6	1,349	6.9956	86.1	174.3
Mean		**2.0**±0.4	**25.78**	**39.91**	**2/2**		**42.8**	**3.2**	**10.3**	**592**	**1.9983**	**87.0**	**147.9**
Basalt of Ithnayn													
R17DC012	0907B	13.5±2.7	26.3419	39.8592	8/8	Li	15.4	4.4	1.3	1,764	7.9960	71.0	206.3
Young basalt east of Ithnayn													
R17DC013	0987B	6.0±1.0	26.3903	40.0701	7/8	Li	30.8	0.5	1.4	1,934	6.9969	80.2	217.3

[a]Code is the project unique site identifier.

[b]Site ID is the field and laboratory identifier.

[c]Ages are $^{40}Ar/^{39}Ar$ and ^{36}Cl exposure ages and one standard deviation uncertainties for samples from the same map unit; see Stelten and others (2020) for full details on age measurements.

[d]Latitude and longitude are site location in degrees north and east in the World Geodetic System of 1984 (WGS 1984) datum.

[e]N/N_o is the number of core samples used in site mean statistics over the number of core samples taken at each site.

[f]Treatment is the nature of the alternating-field (AF) demagnetization used to obtain the site mean direction, where Li is lines solution, Pl is planes solution, and Mx is a mixture of lines and planes solution (Kirschvink, 1980). Th indicates that thermal demagnetization was used.

[g]Inclination is the site mean inclination value in degrees from horizontal (positive is normal, negative is reversed).

[h]Declination is the site mean declination value in degrees east of north.

[j]α95 is the limit of 95 percent confidence about the mean site direction, in degrees.

[k]k is the Fisher precision parameter.

[l]R is the length of the resultant vector.

[m]Pole latitude and pole longitude are the locations in degrees north and east of the site virtual geomagnetic pole.

[n]Sites are thought to have erupted nearly contemporaneously based on unit mean virtual geomagnetic pole directions. See text and table 2 for details. Means of ages are averages of measured values, each weighted by the inverse of its reported uncertainty squared.

Regional archaeomagnetic records from Italy (Vesuvius and Etna) provide good control over the past 2,000 years (Tanguy and others, 2003, 2007; Principe and others, 2004). Archaeomagnetic control for Italy was extended back an additional 1,500 years by Tema and others (2006), whereas paleosecular variation of sediment cores from a maar lake and the adjacent Ionian and Tyrrhenian Seas by Vigliotti (2006) offers a record spanning the entire Holocene. Similarly, archaeomagnetic data collected by Kovacheva (1997) and Kovacheva and others (2009) in Bulgaria are the geographically closest sources of abundant and precise age (or archaeomagnetic) control.

These site records, when compared to similar results from France and the United Kingdom, demonstrate subtle gradients in VGP positions for northwestern Europe compared to southeastern Europe. These gradients can be extended to Harrat Rahat to improve our local geomagnetic secular variation model through the Holocene. In particular, the gradients suggest that the closest, most complete record of secular variation best serves as an archaeomagnetic calibration reference. A record of archaeomagnetic secular variation from the nearby area of Israel/Palestinian Territories was recently published (Shaar and others, 2018). Although the calibration record it offers is spatially close to Harrat Rahat, gaps in that record limit its utility as a calibration reference. We employ the Bulgarian record of Kovacheva and others (2009) as our calibration source because of the record's completeness and areal proximity to our study area.

$^{40}Ar/^{39}Ar$ Dating

One hundred and fifty rock samples were analyzed successfully from throughout the study area for eruption age determinations via the $^{40}Ar/^{39}Ar$ method as part of the Saudi Geological Survey and U.S. Geological Survey. geologic mapping and eruptive history efforts. Results for these 150 samples are presented by Stelten and others (2020), 2023a,b and Stelten (2021). Some of these $^{40}Ar/^{39}Ar$ ages are reported in this chapter (tables 1, 2). Additionally, three new samples were analyzed via the $^{40}Ar/^{39}Ar$ method to support this manuscript and are presented in table 3. Methods and details of sample selection, processing, and Ar isotopic analysis are reported in those publications.

^{36}Cl Cosmogenic Surface-Exposure Dating

Eruption ages were determined by the ^{36}Cl cosmogenic surface-exposure method for mafic lava flows that were either too young to date precisely via the $^{40}Ar/^{39}Ar$ method or in cases where erosional incision was insufficient to expose coarsely crystallized lava interiors fully for $^{40}Ar/^{39}Ar$ dating. For most samples, crushed whole rock was used for ^{36}Cl dating, but plagioclase was analyzed from some sites where loose megacrysts littered the surfaces of young lava flows or where plagioclase megacrysts could be chipped easily from lava flow surfaces with pristine eruptive features, such as glassy pāhoehoe ropes. Eleven samples were successfully measured for ^{36}Cl exposure ages from within our study area. Results for these samples are reported by Stelten and others (2018, 2023a,b) and Downs and others (2018, 2023), and sample preparation and analytical methods are presented in those reports. Some of these ^{36}Cl surface-exposure ages are reported in this chapter (tables 1, 2).

Results

The dominant orientation of remanent magnetization found from our sample sites in Harrat Rahat was a normal polarity centered on an axial dipole direction with inclination of 42° and a declination of 0° (table 1). A combination of field observations, $^{40}Ar/^{39}Ar$ eruption ages, rock chemistry, and paleomagnetic directions allowed the exposed volcanic rocks of northern Harrat Rahat to be subdivided broadly into 12 stages of eruptive activity distinguished as periods of greater or lesser numbers of identified eruptions. The older stages are likely to be composites, since concealment by younger volcanic deposits and loss of constructional relief by erosion hinder distinguishing, or even accessing and therefore sampling and dating, the older eruptive products. Only three exposed volcanic deposits defined independently by field relations and geochronology were found through paleomagnetic study to have reversed polarity, and only six units were designated (by Downs and others, 2019, and Robinson and Downs, 2023) to be part of the oldest exposed eruptive stage (stage 12), and thus greater than 780 ka, and old enough to record reversed polarity. The scarcity of reversed polarity surface outcrops indicates a productive volcanic effusion rate over the past few hundred thousand years which effectively covered the earlier reversed polarity flows presumed to underlie the younger flows. However, a small, unnamed basalt vent in the southern part of the city of Al Madīnah was found to record an ordinary reversed polarity magnetization. Thus, the normal polarity lava flow cover may be thin, particularly in the younger, northernmost part of Harrat Rahat (Camp and Roobol, 1991). In the future, paleomagnetic studies from vertical drill cores to basement, taken down the axis of northern Harrat Rahat, would greatly clarify the long-term eruptive history, including numbers of eruptive episodes, eruptive recurrence rates, depth to reversed polarity flows, and total thicknesses and compositions of volcanic products from northern Harrat Rahat.

Historical 1256 C.E. (654 A.H.) Flow

Paleomagnetic research of northern Harrat Rahat began with an experiment on outcrops of the historical basalt of Al Labah lava flow that extends about 22–23 km in a south to north direction along the presently urbanized eastern margin of Al Madīnah. Observations of this eruption recount its emplacement over 52 days, and examination of the resulting 0.5 km^3 of eruptive products indicate multiple

Table 2. List of mapped volcanic deposits in Harrat Rahat grouped based on close or overlapping $^{40}Ar/^{39}Ar$ or ^{36}Cl ages and similar paleomagnetic directions, suggesting common eruptive episodes with durations of less than two centuries.

[Eruptive stages and geologic unit names and labels from Downs and others (2019) and Robinson and Downs (2023). ka, kilo-annum or thousand years before present]

Eruptive stage	Age	Units in group
Eruptive Stage 2 (11 to 45 ka)	24.6±1.2	Basalt of Southern Fingers (unit bsof), basalt of Northern Fingers (unit bnof), basalt of Central Finger (unit bcef)
Eruptive Stage 4 (70 to 100 ka)	~90 ka	Flows proximal to the mugearite of Hill 1125 vent (unit mh11) and basalt of Sha'ib Al Khakh (unit bsk)
Eruptive Stage 4 (70 to 100 ka)	~82 ka	Trachyte of Gura 5 (unit tg5) and trachyte of Gura 4 (unit tg4)
Eruptive Stage 5 (100 to 180 ka)	~115 ka	Basalt of Shai'ab Abu Sikhbir (unit bsas) and mugearite of Dabaa 1 (unit md1)
Eruptive Stage 5 (100 to 180 ka)	~145 ka	Basalt of Hill 1066 (unit bh10) and basalt of Sha'ib Iskabah (unit bsi)
Eruptive Stage 5 (100 to 180 ka)	~145 ka	Basalt of Al Khanaq (unit bka) and basalt of Ash Suqayyiqah (unit bsq)
Eruptive Stage 6 (180 to 260 ka)	~193 ka	Basalt of Ar Rummanah (unit bru), basalt of Al Jassah (unit bjs), basalt of Shuran (unit bsh), and mugearite of Um Zhabah 2 (unit mz2)
Eruptive Stage 6 (180 to 260 ka)	~217 ka	Basalt of Qa Al Ghusun (unit bqg) and basalt of Abu Ghuwayshiyah (unit bag)
Eruptive Stage 6 (180 to 260 ka)	~225 ka	Basalt of Banthane Dam (unit bbd) and basalt of Lower Sha'ib Lihyan (unit blsl)
Eruptive Stage 6 (180 to 260 ka)	~235 ka1	Basalt of Sha'ib Hayaya (unit bhy) and basalt of Abu Siyilah (unit bsy)
Eruptive Stage 7 (260 to 323 ka)	~285 ka	Basalt of Al Huzaym (unit bhu) and basalt of An Nughayr (unit bau)
Eruptive Stage 9 (360 to 460 ka)	~380 ka	Basalt of Powerline Road (unit bpr) and basalt of Al Harrah Al Gharbiyah (unit bhg)
Eruptive Stage 9 (360 to 460 ka)	~400 ka	Mugearite of Um Znabah 3 (unit mz3), mugearite of Um Znabah 6 (unit mz6), and trachyte of Um Znabah 6 (unit tz6)
Eruptive Stage 9 (360 to 460 ka)	~415 ka	Benmoreite As Zayinah (unit ozy) and basalt of Rahat (unit brh)
Eruptive Stage 10 (460 to 570 ka)	~510 ka	Basalt of Upper Sha'ib Huquf (unit buph) and basalt of Al Farash (unit bfa)
Eruptive Stage 10 (460 to 570 ka)	~545 ka	Basalt of Al Ihn (unit bai) and basalt of Um Rgaibah (unit brg)

phases of flow emplacement, first toward and then flanking the then-established city of Al Madīnah (Camp and others, 1987). The purpose of the paleomagnetic experiment was to test if (1) multiple outcrops of this basalt flow share a single remanent direction of magnetization and (2) that its single mean direction of magnetization matches directions expected for its eruption age by comparison with a calibrated record of local secular variation. We sampled three separate sites within this 1256 C.E. lava flow. They were in positions proximal to the main vent alignment, 3 to 5 km from the vents, and in the far northern extent of the lava flow. Results from those three sites are given in table 1 and are shown on figure 3. The paleomagnetic results from the three sites group well in a shallow, easterly direction of magnetization, with a kappa value exceeding 5,000 and an α95 value of 1.7°, both indicating close agreement among the sites. The kappa value is an inverse measure of sample dispersion (in which a high value indicates closer consistency than a low value), and α95

is the radius in degrees of the 95 percent confidence limit centered on the mean direction of remanent magnetization.

We assess the mean remanent direction for the historical basalt of Al Labah by converting to its VGP and then calculating the direction that VGP would produce at Sofia, Bulgaria. This allows our local magnetic direction to be compared with the 8,000-year-long record of geomagnetic secular variation assembled for Bulgaria (fig. 4). In figure 4, the time of the 1256 C.E. eruption is shown as a dashed blue vertical line, and the inclination and declination (52° and 9°, respectively) suggested for Sofia, Bulgaria, from our average basalt of Al Labah direction transformed through the VGP is also shown. The calculated magnetic direction for Bulgaria around 1256 C.E. closely matches our transformed direction from the basalt of Al Labah. This match supports the conclusion that the three sites within the 1256 C.E. lava flow are not only well grouped and precise, but also quite accurate in their average remanent direction.

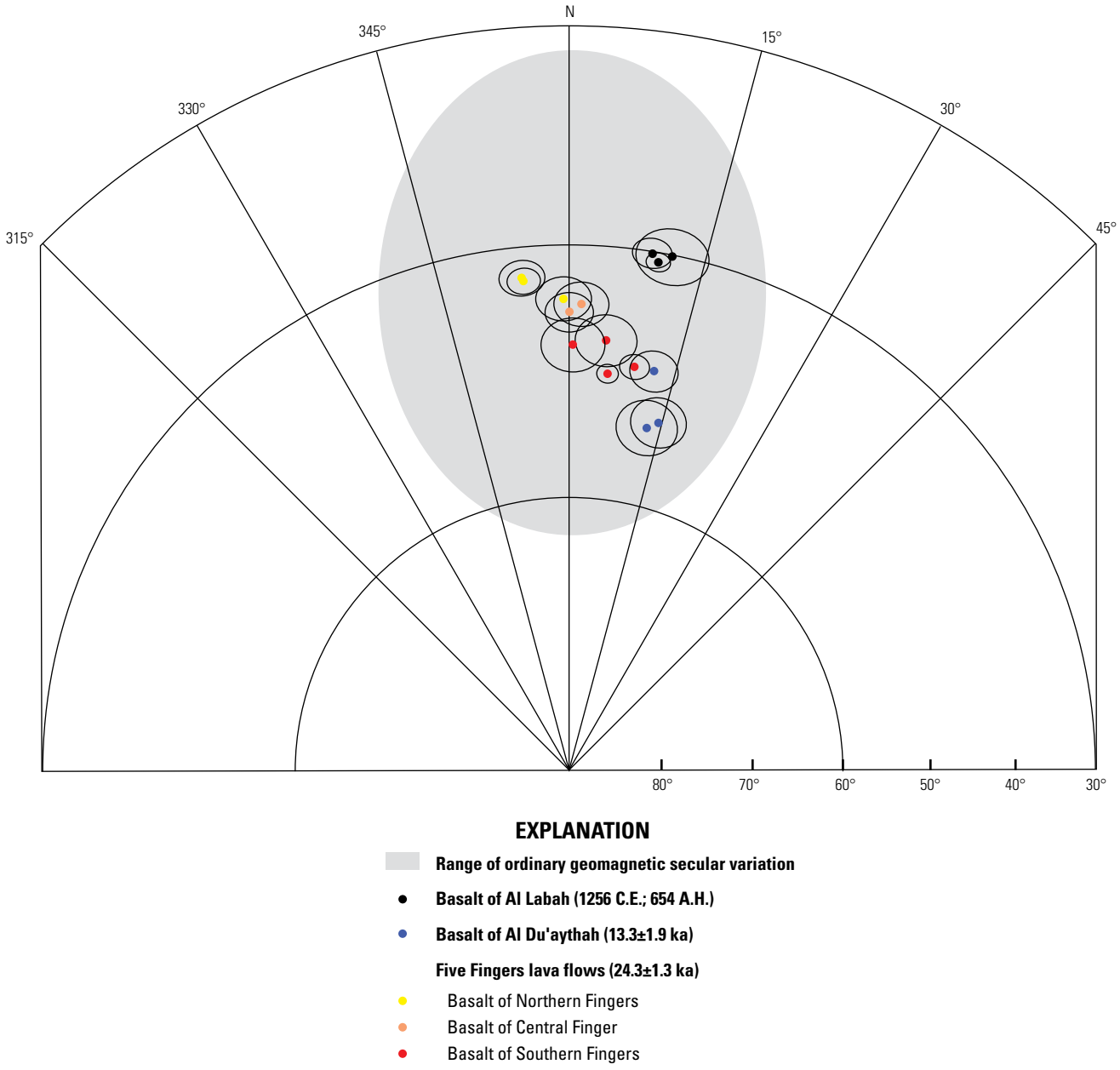

Figure 3. Northern part of a lower hemisphere equal-area plot showing mean directions of remanent magnetization and enclosing 95 percent confidence envelopes (black ellipses) for sampled sites in northern Harrat Rahat. Geologic units shown are the basalt of Al Labah (1256 C.E., 654 in the year of the Hijra [A.H.]), basalt of Al Du'aythah (13.3±1.9 kilo-annum [ka]), and three basalts from the Five Fingers lava flows: basalt of Southern Fingers, basalt of Northern Fingers, and basalt of Central Finger—all dated to 24.6±1.2 by ^{36}Cl surface-exposure dating.

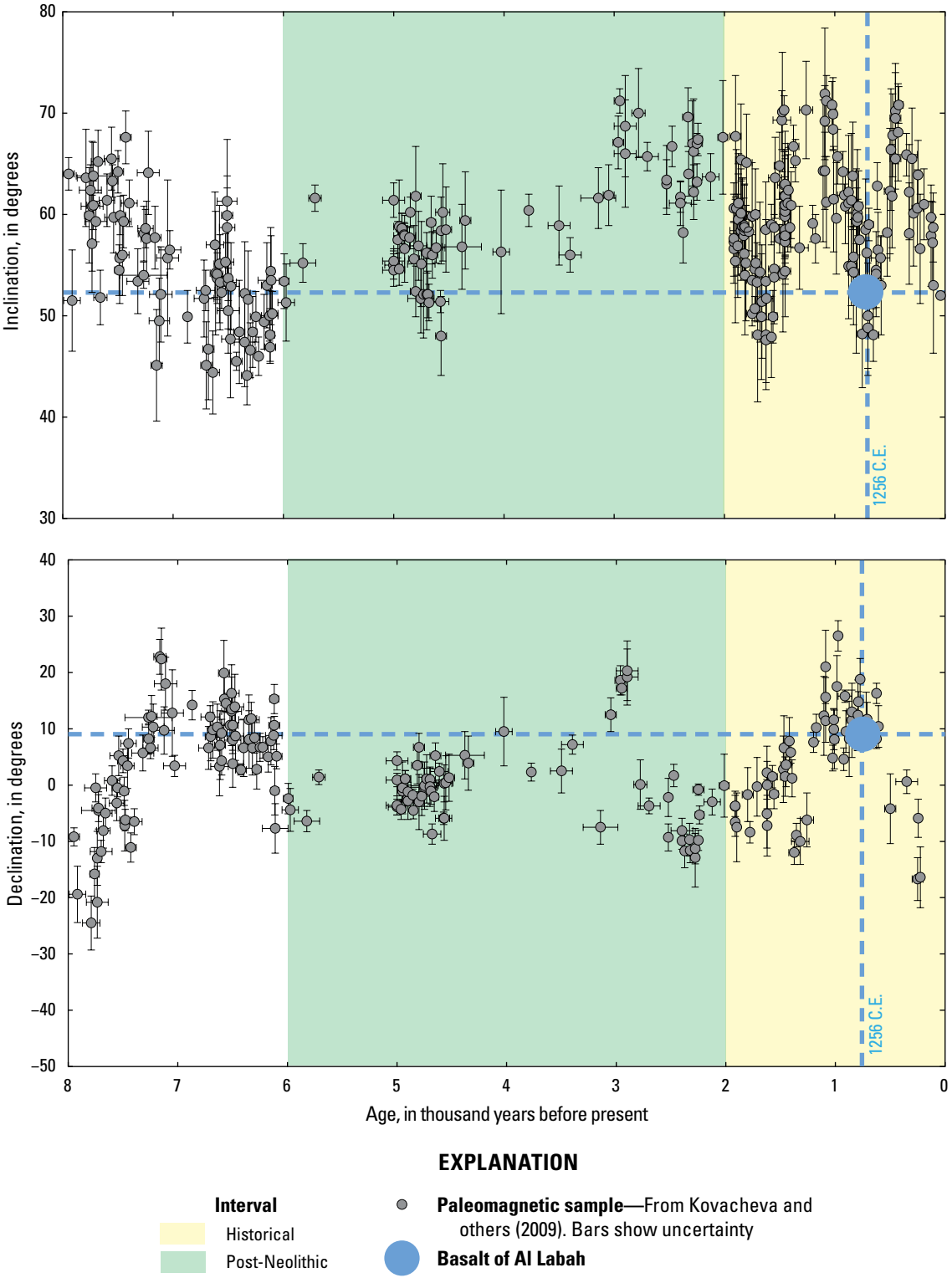

Figure 4. Plot of archaeomagnetic inclinations and declinations spanning the past 8,000 years from Bulgaria (Kovacheva and others, 2009) compared to the remanent magnetic direction for the historical basalt of Al Labah (1256 C.E., 654 in the year of the Hijra [A.H.]), converted through its virtual geomagnetic pole transformation to the location of Sofia, Bulgaria. The thus converted paleomagnetic direction for the 1256 C.E. lava flow matches the magnetic direction in Bulgaria for that age.

641 C.E. (20 A.H.) Eruption

An aligned group of four young-appearing cinder cones with stubby lava flows located in the southwestern fringe of Al Madīnah were postulated to have erupted in 641 C.E. (20 A.H.) (Camp and Roobol, 1989, 1991) based on a comment of an eruption in the greater Al Madīnah area in that year (Al-Samhūdī, 1488). The cones were identified as the youngest volcanic deposits near to Al Madīnah, other than those of the 1256 C.E. eruption, based on a combination of remote sensing imaging and lack of erosional incision. The historical report, however, was written nearly 850 years after the eruption, presumably based on earlier documents that have been lost, and the account distinctly lacks specifics. Murcia and others (2015) further discuss the character and age attribution of these four cinder cones, and named them the Al Du'aythah volcanic cones, after the neighborhood in which they are located. They also acknowledge that different historical records present conflicting information as to the location of the 641 C.E. eruption, and finally state that these cones are young, and likely Holocene.

We conducted paleomagnetic field sampling on the Al Du'aythah cones, collecting samples from three sites at three of the four cones (fig. 3 and table 1). These sites record similar mean remanent directions of magnetization with inclination values near 50.5° and declination values near 13.5°. Their similar magnetic directions indicate that they were constructed in a single eruptive episode of short duration (likely less than a century). Murcia and others (2015) also suggested a brief continuous eruption in three eruptive phases and noted minimal evidence of chemical variation in samples from the Al Du'aythah cones and small lava flows, unlike the other young flows from northern Harrat Rahat, such as the 1256 C.E. eruption and the basalts of Northern Fingers, Central Finger, and Southern Fingers (commonly referred to as the "Five Fingers").

To test the postulated 641 C.E. age assignment of the Al Du'aythah cones, we compared its mean remanent direction against the calibrated record of geomagnetic secular variation from Bulgaria in a manner similar to our comparison of the 1256 C.E. results. Our local mean direction for the three sites in Al Du'aythah converts to an inclination of 64° and a declination of 19° in Sofia, Bulgaria. Compared to the Bulgarian geomagnetic curve, we see that although the inclination value agrees, the declination value is too high for 641 C.E. (fig. 5). Declinations as easterly as 19° are not common as is documented for the past 8,000 years in Bulgaria. The mismatch in declination is strong evidence that the Al Du'aythah cones did not erupt in 641 C.E. A subsequent ^{36}Cl cosmogenic surface-exposure age of 13.3±1.9 ka conclusively established that the cones did not erupt in 641 C.E., and that they are slightly older (Downs and others, 2018; Stelten and others, 2020). The ^{36}Cl age does confirm that Camp and Roobol (1989, 1991) correctly identified that the Al Du'aythah cones are the youngest eruptive products to have vented close to Al Madīnah other than those of the 1256 C.E. event.

The location of the 641 C.E. eruption is possibly answered by results we obtained from a lava flow in the Harrat Khaybar volcanic field to the north, from which we collected three paleomagnetic and ^{36}Cl cosmogenic surface-exposure age samples (table 1). Roobol and Camp (1991) interpreted eight lava flows of Harrat Khaybar as potentially having erupted in historical times, based on stratigraphic position, lack of erosion or sediment cover, lack of anthropogenic structures, and on aspects of remote sensing images. The largest of these are the basaltic cone, lavas, and scoriae apron of Jabal Qidr at the crest of the harrat, and the 55-km-long Habir basaltic lava flow that descended west from the crest nearly to the ancient community of Khaybar. The other potentially historical flows are much smaller and are restricted to the crest of the harrat. Roobol and Camp (1991) supported a historical age for the Habir flow with the observation that it overrode and banked against Neolithic stone structures, and they reference Burton (1879) who recounted a report of an eruption from Harrat Khaybar "in the time of the Prophet's successor, Omar" (634–644 C.E.). Two sites in the 55-km-long basaltic Habir lava flow produced paleomagnetic data indicating a mean inclination of 43° and mean declination of 3°. This value, when converted through its VGP to the location of Sofia, Bulgaria, falls on that calibration curve at a time of 600–700 C.E., as well as several earlier times (fig. 6). The Habir flow lies approximately 100 km closer to the location of the principal historical observation point of the 641 C.E. eruption (Al-Samhūdī, 1488), and the flow is much larger than the small cones and flows of the basalt of Al Du'aythah in western Al Madīnah. The community of Khaybar lay on the commonly traveled route from Damascus and the Levant to Al Madīnah (formerly known as Yathrib), and from there to Makkah and Jiddah, so a large lava flow approaching the settlement over weeks or months would have been observed widely and reported in nearby Al Madīnah, but specific details were likely lost in the 850 years from the eruption to its final recording by Al-Samhūdī (1488).

Cosmogenic surface-exposure ages using ^{36}Cl were generated from samples collected at five locations within Harrat Khaybar and Harrat Ithnayn, the harrat adjacent to the north of Harrat Khaybar (table 1). The uncertainty-weighted average ^{36}Cl cosmogenic surface-exposure age for the Habir flow of 2.0±0.4 ka (1σ) is somewhat older than the approximately 1,380 years since 641 C.E. but overlaps it at the two standard deviation (2σ) level. The Qidr eruption may also occur in the same timeframe as it records a similar mean direction of remanent magnetization, and a similar ^{36}Cl exposure age of 1.8±0.4 ka (1σ). Taken together with the paleomagnetic data, this age assessment for the Habir and Qidr flows offers a strong possible location for the historically documented eruption on the Arabian Peninsula at 641 C.E.

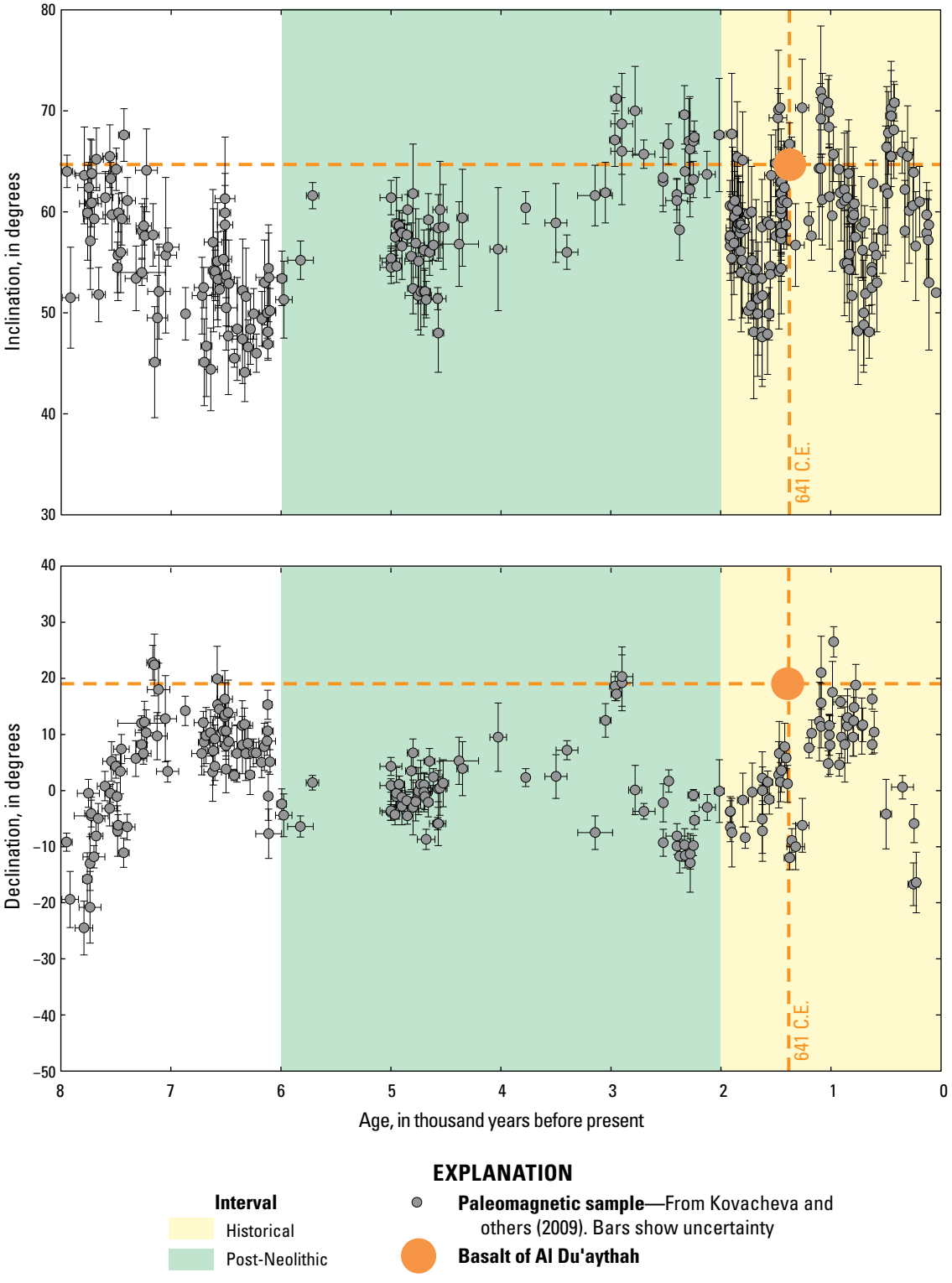

Figure 5. Plot of archaeomagnetic inclinations and declinations spanning the past 8,000 years from Bulgaria (Kovacheva and others, 2009) compared to the remanent magnetic direction for the basalt of Al Du'aythah, converted through its virtual geomagnetic pole transformation to the location of Sofia, Bulgaria. The declination in Bulgaria at 641 C.E. does not match that of the basalt of Al Du'aythah translated to the same location, indicating that those small cones and flows did not erupt in 641 C.E.

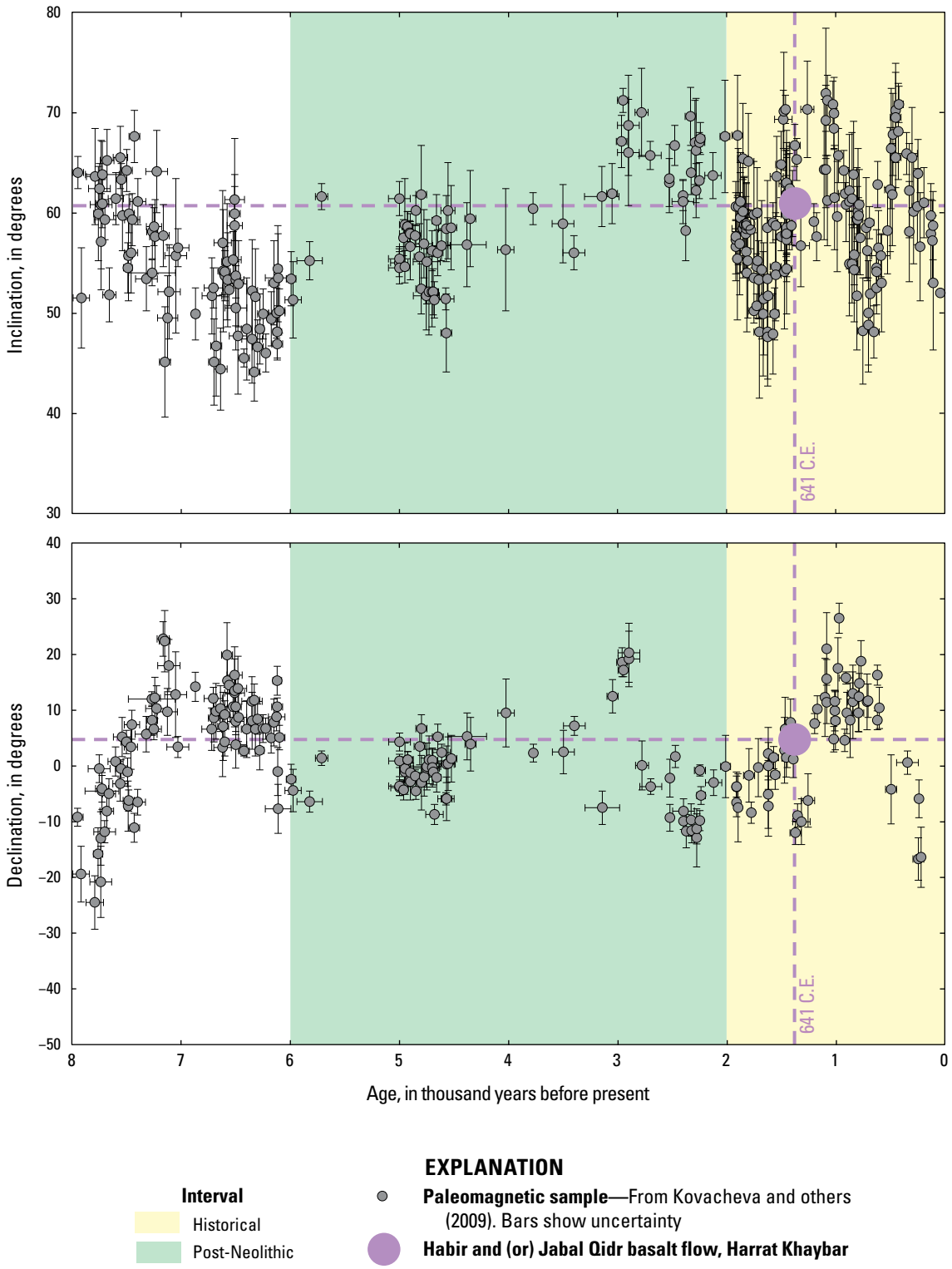

Figure 6. Plot of archaeomagnetic inclinations and declinations spanning the past 8,000 years from Bulgaria (Kovacheva and others, 2009) compared to the remanent magnetic direction for the Habir basalt flow of Harrat Khaybar (Roobol and Camp, 1991), converted through its virtual geomagnetic pole transformation to the location of Sofia, Bulgaria. The paleomagnetic directions at 600–700 C.E. in Bulgaria match that of the Habir flow translated to the same location, supporting that effusion of the Habir lava flow was the eruption documented to have taken place in 641 C.E. (20 in the year of the Hijra in the greater Al Madīnah region.

Five Fingers Lava Flows

The Five Fingers lava flows (Murcia and others, 2016; Moufti and Németh, 2016; Dietterich and others, 2018; Downs and others, 2019; Robinson and Downs, 2023) are a cluster of sizeable, young appearing (black and nearly sediment free) flows of basalt that erupted from near the northern end of the topographically high axis of vents that defines the crest of northern Harrat Rahat. The flows then traveled north, northeast, and east into presently unpopulated areas. The flows formed in three eruptions with superposition showing that the first eruption formed the single lava stream of the Central Finger, followed by eruptions of the Northern and Southern Fingers, each of which produced two lava streams (Camp and Roobol, 1991; Downs and others, 2019; Robinson and Downs, 2023). The basalts of Northern and Southern Fingers are not in contact, so their relative ages are unknown from field relations. Proximity and alignment of vents, similar low degrees of weathering and sediment cover, and partial overlap of chemical compositions support eruption of the Five Fingers lavas in a short time interval but of unknown duration. These flows were previously interpreted as post-Neolithic (<6 ka) owing to an absence of stone structures upon them that were constructed throughout the area during a period of enhanced rainfall and accompanying relatively high Neolithic human populations (Camp and Roobol, 1991). Hyper-arid conditions followed this Neolithic pluvial period with consequent severe reductions in animal and human populations and abandonment of the construction of stone structures. New ^{36}Cl surface-exposure dating, however, determined ages for the basalts of Northern Fingers, Central Finger, and Southern Fingers ranging from 29.1±3.7 to 22.0±3.3 ka, well before the Neolithic pluvial period (Stelten and others, 2020, 2023a). Paleomagnetic sampling of lava flow outcrops from these eruptive units (table 1) reveals that they do not share the same mean directions of remanent magnetization, indicating that at least several centuries separated their eruptions. Figure 3 shows the average remanent directions and enclosing 95 percent confidence limits for nine sites sampled in the Five Fingers lava flows (table 1). Although these individual magnetizations differ, they are close to one another and describe a continuous trend that suggests a single, relatively short eruptive timespan. The nine site averages represent a limited variation compared to the extent of possible directions of magnetization owing to geomagnetic secular variation (gray area on fig. 3). Because of the limited extent of directional variation, we use a weighted mean age of 24.6±1.2 ka for the eruption age of all three units but recognize that there may have been several centuries between their eruptions. The Five Fingers lava flows may lack Neolithic stone structures because their youthful, rugged surfaces were less hospitable than nearby older lavas that have been smoothed by erosion.

Lava Flows within Al Madīnah

Despite long and intensive urbanization within and near Al Madīnah, shaded relief and slope maps developed from light detection and ranging (lidar) digital topography show isolated outcrops and some approximate flow boundaries that guided paleomagnetic sampling and geologic mapping. We sampled 55 sites within the city interior, and when combined with rock chemical compositions and ^{40}Ar/^{39}Ar ages, we were able to map the volcanic geology (Downs and others, 2018). We find lava flows from 25 separate eruptions cross the Third Ring Road (King Khalid Road) generally from vent sites to the south and south-southeast. Should similar eruptions occur in the future, they would threaten inhabited and developed areas of the city of Al Madīnah. These lava flows have eruption ages that span from older than 780 ka to historical.

Identifying Brief Eruptive Episodes in Harrat Rahat

A fundamental motivation for carrying out paleomagnetic field studies of northern Harrat Rahat was the expectation we would discover, and correlate, brief periods of temporally clustered eruptions. Stratigraphic position, geochemical compositions, and isotopic ages each support, to different degrees, our hypothesis that some eruptions were clustered temporally but separated geographically. Geochronology by the applied ^{40}Ar/^{39}Ar and ^{36}Cl cosmogenic surface-exposure methods, however, is generally insufficiently precise to establish contemporaneity more narrowly than within a few thousand years. Earth's magnetic field drifts rapidly enough that if two or more separate vents or lava flows share similar (within uncertainty) remanent directions of magnetization, their eruptions could have been separated by no more than several hundred years or less. The magnetic field has assumed similar configurations many times over Earth's history, so similar or near-identical remanent directions of magnetization in rocks are necessary, but not sufficient, to establish contemporaneity. If other evidence concurs, such as similar degrees of erosion, stratigraphic position, or absolute age determinations, then the closer the remanent directions of magnetization, the greater the likelihood that eruptions were nearly contemporaneous. We were thus able to identify numerous brief episodes when more than one vent and lava flow are time correlative and demonstrate that they may or may not share the same geochemistry.

In part by using this paleomagnetic demonstration of time groups, Stelten and others (2023a) described a mixed exponential model that derives two characteristic states of the magmatic system, one in which eruptions were separated by an average of 4,000 years, and another in which the intervals between eruptions were brief, averaging 220 years (the average duration of this short interval is not narrowly defined by the measured ages). In practice, this suggests long-term reposes between eruptions that average 4,000 years, but that once one eruption has happened, the probability remains elevated for another eruption within the next several centuries. This mixed exponential model yields a probability of 0.11 percent for an eruption in the year following an eruption, or slightly more than four times the long-term eruption probability of about 0.025 percent per year, falling to

0.08 percent per year after a century and 0.05 percent per year after 300 years, still double the long-term rate (Stelten and others, 2023a). Enough time has passed since the 1256 C.E. eruption that the estimated probability of eruption near Al Madīnah is now indistinguishable from the long-term rate (Stelten and others, 2023a). This second eruption need not be of the same magma composition, its vent complex need not be aligned with that of the first, and the vents need not be particularly close. The eruptive hazard profile of northern Harrat Rahat is thus enhanced with the understanding that once an eruption begins in the volcanic field, the likelihood is greater—although still low—that another vent may open and produce lava flows within a few centuries, and that vent may be distant from any other eruption that is part of the eruptive episode. In a geologic context, the mixed exponential model suggests the occurrence of a volcanic eruption within northern Harrat Rahat is not necessarily the result of a single magma being injected into the crust and erupting. Instead, the occurrence of an eruption may more broadly indicate that the magmatic system is entering a more active phase and future eruptions may occur.

Sixteen paleomagnetically correlated eruptive episodes that we identified in the northern Harrat Rahat study area are listed and briefly described below from youngest to oldest. All geologic unit names, labels, and ages are from Downs and others (2019) and Robinson and Downs (2023) and build on the nomenclature and stratigraphy established by Moufti (1985).

1. We described herein an episode of correlative eruptions of the basalt of Southern Fingers (unit bsof), basalt of Northern Fingers (unit bnof), and the basalt of Central Finger (unit bcef) in our discussion of the youngest units of Harrat Rahat (fig. 3). Although these three units do not share identical remanent directions, their similarity and the overlapping nature of their uncertainty weighted averaged ^{36}Cl cosmogenic surface-exposure ages (24.6±1.2 ka) are interpreted to represent an eruptive timeframe of only a few centuries (tables 1, 2).

2. The mugearite of Hill 1125 (unit mh11) and the basalt of Sha'ib Al Khakh (unit bsk) share a shallow inclination and somewhat westerly direction of remanent magnetization that are indistinguishable at the 95 percent confidence level (fig. 7*A*; tables 1, 2). The mugearite of Hill 1125 records two separable remanent magnetic directions, suggesting that, as mapped, it may encompass the products from two eruptions in which differences were overlooked during field studies. Half of its measured sites match the basalt of Sha'ib Al Khakh. This is the youngest example of an eruptive episode composed of geochemically dissimilar magmas. Neither of these units are dated by the ^{40}Ar/^{39}Ar method, but age measurements from overlying and underlying stratigraphic units indicate an age of ~90 ka for this eruptive episode.

3. The tuffs of the trachytes of Gura 5 (unit tg5) and Gura 4 (unit tg4) share a steep inclination and far westerly direction of remanent magnetization that are barely distinguishable at the 95 percent confidence level (fig. 7*A*). They vented from nearby craters of the same eruptive center and have similar ^{40}Ar/^{39}Ar ages of 79.7±1.6 and 84.3±1.6 ka, respectively, and both overlie the trachyte of Al Efairia (unit tef), which has an ^{40}Ar/^{39}Ar age of 88.0±1.8 ka (Moufti, 1985; Stelten and others, 2020) (tables 1, 2). This episode is thus dated just older than ~80 ka.

4. The basalt of Sha'ib Abu Sikhbir (unit bsas) and the mugearite of Dabaa 1 (unit md1) share a slightly shallow inclination and northerly direction of remanent magnetization that are indistinguishable at the 95 percent confidence level (fig. 7*A*; tables 1, 2). In addition, they share overlapping ^{40}Ar/^{39}Ar ages of 115.3±7.5 and 116.7±2.8 ka. Thus, despite their dissimilar compositions, they indicate a common eruptive episode at ~115 ka.

5. The basalt of Hill 1066 (unit bh10) and the basalt of Sha'ib Iskahab (unit bsi) share a shallow, northerly direction of remanent magnetization that is indistinguishable at the 95 percent confidence level (fig. 7*A*; tables 1, 2). They also have overlapping ^{40}Ar/^{39}Ar ages of 137.3±11.3 and 151.9±9.9 ka. This indicates a common eruptive episode close to 145 ka.

6. The basalt of Al Khanaq (unit bka) and the basalt of Ash Suqayyiqah (unit bsq) share an ordinary inclination value and somewhat westerly direction of remanent magnetization that are barely distinguishable at the 95 percent confidence level (fig. 7*A*; tables 1, 2). The basalt of Al Khanaq has an ^{40}Ar/^{39}Ar age of 144.6±19.6 ka, whereas the basalt of Ash Sugayyiqah is known to be older than 83 ka. Their eruptive timeframe association is weaker than those described above but suggest a possible episode at about 145 ka. Despite similar estimated ages, the different paleomagnetic directions distinguish this from the episode defined by the basalts of Hill 1066 and Sha'ib Iskahab.

7. The basalt of Ar Rummanah (unit bru), the basalt of Al Jassah (unit bjs), and some sites in the mugearite of Um Znabah 2 (unit mz2) share odd shallow inclinations and far easterly directions of remanent magnetization that, in part, document a probable excursion of the local geomagnetic field. In addition, the vent for the basalt of Shuran (unit bsh) shares a similar slightly steeper inclination and northerly declination remanent magnetic direction with other sites from the mugearite of Um Znabah 2 (tables 1, 2). The dispersion of remanent directions in these four volcanic units indicates they were acquired in a quickly changing geomagnetic field,

during a geomagnetic cryptochron timeframe. The units also share similar $^{40}Ar/^{39}Ar$ ages of 191.5±4.2 and 195.9±1.3 ka, indicative of a brief eruptive episode close to 193 ka.

8. The basalt of Qa Al Ghusun (unit bqg) and the basalt of Abu Ghuwayshiyah (unit bag) share an ordinary inclination and far easterly direction of remanent magnetization that are indistinguishable at the 95 percent confidence level, though the site in the basalt of Qa Al Ghusun has large uncertainty (fig. 7*A*; tables 1, 2). They also share overlapping $^{40}Ar/^{39}Ar$ ages of 215.2±6.9 and 220.3±8.3 ka. This indicates they erupted nearly contemporaneously at about 217 ka.

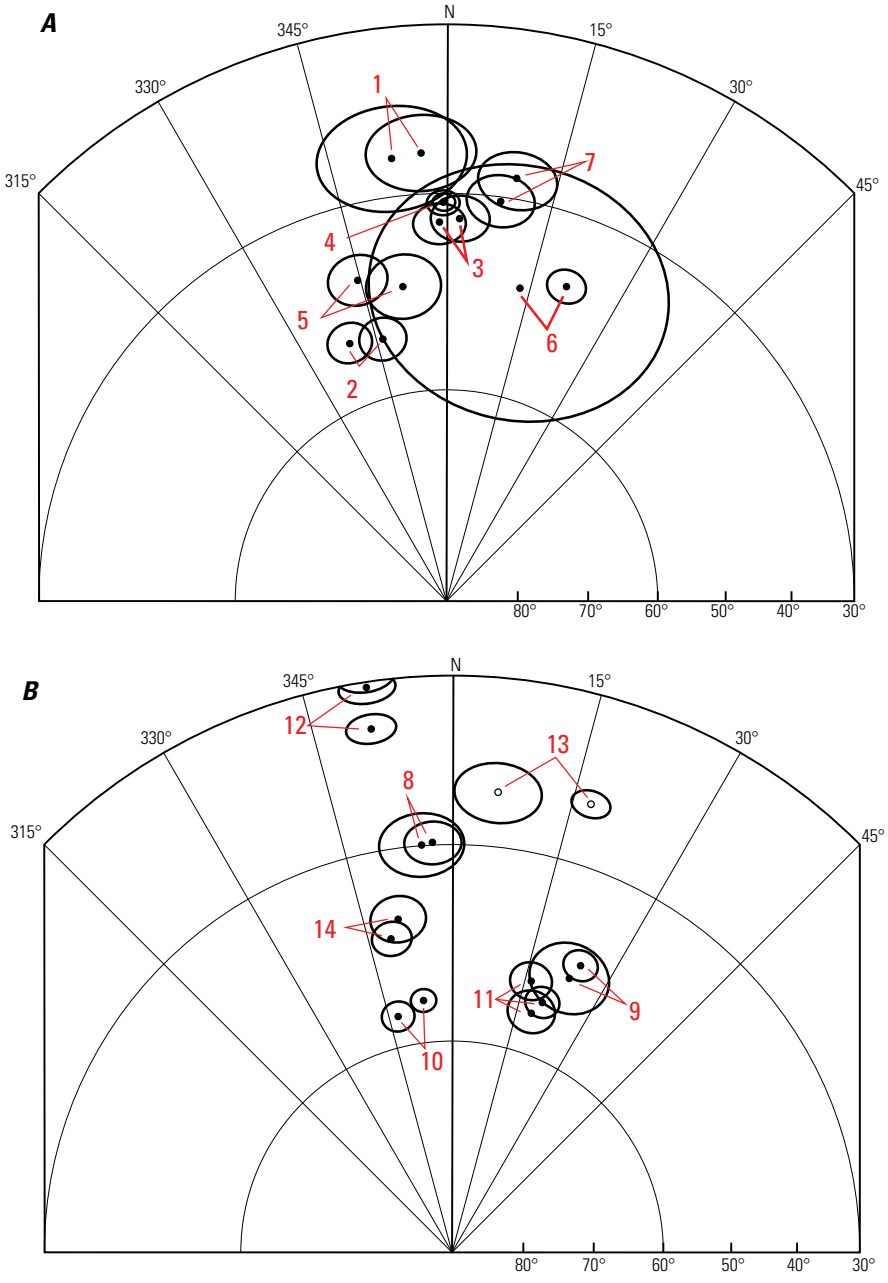

EXPLANATION

Site groupings showing mean directions of remanent magnetization

1. Mugearite of Hill 1125 and basalt of Sha'ib Al Khakh
2. Trachyte of Gura 5 and trachyte of Gura 4
3. Basalt of Shai'ab Abu Sikhbir and mugearite of Dabaa 1
4. Basalt of Hill 1066 and basalt of Sha'ib Iskabah
5. Basalt of Al Khanaq and basalt of Ash Suqayyiqah
6. Basalt of Qa Al Ghusun and basalt of Abu Ghuwayshiyah
7. Basalt of Banthane Dam and basalt of Lower Sha'ib Lihyan
8. Basalt of Sha'ib Hayaya and basalt of Abu Siyilah
9. Basalt of Al Huzaym and basalt of An Nughayr
10. Basalt of Powerline Road and basalt of Al Harrah Al Gharbiyah
11. Mugearite of Um Znabah 3, mugearite of Um Znabah 6, and trachyte of Um Znabah 6
12. Benmoreite of As Zayinah and basalt of Rahat
13. Basalt of upper Sha'ib Huquf and basalt of Al Farash (open symbols mean upper hemisphere)
14. Basalt of Al Ihn and basalt of Um Rgaibah

Figure 7. Northern part of lower hemisphere equal-area plots showing site mean directions of remanent magnetization and enclosing 95 percent confidence envelopes (black ellipses) for sites thought to have erupted penecontemporaneously as determined from their locations, geologic field relations, geochronology, and similar magnetizations. *A*, Site groupings for volcanic deposits younger than about 225 thousand years before present (ka). *B*, Site groupings for volcanic deposits older than about 225 ka. Site groupings are noted in tables 1 and 2.

9. The basalt of Banthane Dam (unit bbd) and the basalt of Lower Sha'ib Lihyan (unit blsl) share a shallow inclination and easterly direction of remanent magnetization that are indistinguishable at the 95 percent confidence level (fig. 7*A*; tables 1, 2). They also share overlapping $^{40}Ar/^{39}Ar$ ages of 223.4±8.6 and 228.6±12.0 ka. This indicates they erupted nearly contemporaneously at about 225 ka.

10. The basalt of Sha'ib Hayaya (unit bhy) and the basalt of Abu Siyilah (unit bsy) share a shallow, slightly westerly direction of remanent magnetization that is indistinguishable at the 95 percent confidence level (fig. 7*B*; tables 1, 2). They also share overlapping $^{40}Ar/^{39}Ar$ ages of 235.1±7.5 and 236.2±29.2 ka. This indicates they erupted nearly contemporaneously at close to 235 ka.

11. The basalt of Al Huzaym (unit bhu) and the basalt of An Nughayr (unit bau) share a somewhat steep inclination and far easterly direction of remanent magnetization that are indistinguishable at the 95 percent confidence level (fig. 7*B*; tables 1, 2). The basalt of Al Huzaym has an $^{40}Ar/^{39}Ar$ age of 285.1±6.6 ka. This indicates a common eruptive episode close to 285 ka.

12. The basalt of Powerline Road (unit bpr) and the basalt of Al Harrah Al Gharbiyah (unit bhg) share a very steep, westerly direction of remanent magnetization that is similar but distinguishable at the 95 percent confidence level (fig. 7*B*; tables 1, 2). They also share overlapping $^{40}Ar/^{39}Ar$ ages of 378.8±10.0 and 382.5±5.8 ka. This indicates they erupted nearly contemporaneously at about 380 ka.

13. The mugearite of Um Znabah 3 (unit mz3), mugearite of Um Znabah 6 (unit mz6), and trachyte of Um Znabah 6 (unit tz6) all share a steep inclination and strong easterly direction of remanent magnetization that are indistinguishable at the 95 percent confidence level (fig. 7*B*; tables 1, 2). They all also share differentiated compositions and are spatially grouped. None of these units have $^{40}Ar/^{39}Ar$ ages, but stratigraphic constraints from overlying and underling units indicate a common age of about 400 ka.

14. The basalt of Rahat (unit brh) and the benmoreite of As Zayinah (unit ozy) share an extremely shallow inclination and westerly directions of remanent magnetization that indicate a common eruption timeframe during a geomagnetic cryptochron (fig. 7*B*; tables 1, 2). They also share overlapping $^{40}Ar/^{39}Ar$ ages of 411.5±5.9 and 418.8±1.9 ka. Thus, their eruptions must have been close to 415 ka.

15. The basalt of Upper Sha'ib Huquf (unit buph) and the basalt of Al Farash (unit bfa) share unusual shallow, upper hemisphere inclinations and northeasterly directions of remanent magnetization that indicate both erupted during a particular geomagnetic cryptochron (fig. 7*B*; tables 1, 2). The basalt of Upper Sha'ib Huquf has an $^{40}Ar/^{39}Ar$ age of 510.8±29.4 ka, so both basalts probably erupted around that time.

16. The basalt of Um Rgaibah (unit brg) and the basalt of Al Ihn (unit bai) share ordinary inclinations and westerly directions of remanent magnetization that are indistinguishable at the 95 percent confidence level (fig. 7*B*; tables 1, 2). They also share overlapping $^{40}Ar/^{39}Ar$ ages of 543.3±5.6 and 546.2±9.6 ka. This indicates that both basalts erupted at about 545 ka.

Geomagnetic Excursions Recorded at Harrat Rahat

Among the 173 paleomagnetic sites sampled within Harrat Rahat, 13 have mean remanent directions of magnetization that plot at, or outside, the boundary surrounding the range of ordinary secular variation. This boundary is here defined at a colatitude value of 22° for the site VGP. These anomalous directions were acquired by lava flows that erupted during geomagnetic cryptochrons when the geomagnetic field underwent an excursion from its typical orientation. Approximately every 15,000 to 30,000 years, the geomagnetic field deviates from its ordinary polarity and moves toward opposite polarity in a brief time interval of 500 to 1,500 years. Oda (2005) first tabulated the age pattern of many of these excursions through the study of marine sediments and documented global evidence for more than 20 cryptochrons during the Brunhes Normal Polarity Chron. A more recent compilation by Channell and others (2020) is the most complete that is available at the present time, but additional cryptochrons are also likely to be identified in the future. Remanent magnetic directions outside ordinary secular variation limits occur somewhat less than 10 percent of the time, but they offer both strong opportunity for lava flow correlation and the possibility of providing supporting age control.

Establishing at what degree of angular divergence a mean remanent magnetic direction is anomalous requires an explanation. The standard of ordinary behavior used by the paleomagnetic community for decades is of a site VGP paleolatitude that is equal to or lower than 45° (colatitude greater than or equal to 45°, after Verosub and Banerjee [1977]). No particular philosophical guidance was provided for this definition, except that it was already in common use at the time. We speculate that the definition arises from considering VGP paleolatitudes near ±90° to be normal or reversed polarity, paleolatitudes near 0° to be transitional, and the equant latitude boundary between those two conditions to be ±45°. Historical data from geomagnetic observatories and archaeomagnetic databases do not come close to the 45° VGP boundary, suggesting that it is an overly large definition of ordinary geomagnetic secular variation. We conclude that the 45° VGP colatitude limit to define ordinary geomagnetic secular variation is ill defined and too large; we instead use a

colatitude limit of 22° to define an excursion from ordinary geomagnetic secular variation that was acquired during a geomagnetic cryptochron.

Using this criterion, we identify 13 episodes of anomalous remanent directions recorded in northern Harrat Rahat lava flows that erupted during the Brunhes Normal Polarity and latest Matuyama Reversed Polarity Chrons. We list those episodes below from youngest to oldest and, where possible, we correlate them to the global Oda (2005) and Channell and others (2020) compilations for named cryptochrons. Geologic unit names and labels are from Downs and others (2019) and Robinson and Downs (2023).

1. The hawaiite of Khamisah (unit hkh) records an excursional remanent direction with steep inclination, far westerly declination, and a colatitude value of 34° (fig. 8). It is located just south of the study area but was included in the map and descriptions of Downs and others (2019) and Robinson and Downs (2023). The $^{40}Ar/^{39}Ar$ age for the hawaiite of Khamisah is 29.0±3.9 ka, which overlaps the age of the Auckland Cryptochron at ~31 ka and suggests it correlates to that brief event (Laj and others, 2014; Leonard and others, 2017). The Auckland Cryptochron was previously named the Mono Cryptochron, using paleomagnetic and erroneous ^{14}C age data from rhyolite ashes deposited in Mono Lake, California. More recently acquired ^{238}U-^{230}Th and $^{40}Ar/^{39}Ar$ ages (Marcaida and others, 2019) document that those deposits correlate to the Laschamps Cryptochron.

2. The basalt of Nashbah (unit bns) records an excursional remanent magnetic direction with somewhat shallow inclination, far easterly declination, and a colatitude value of 22°, just at the limit of ordinary geomagnetic secular variation (fig. 8). The $^{40}Ar/^{39}Ar$ age for this unit is 134.1±24.3 ka (table 3), which loosely correlates to the Albuquerque Cryptochron of Oda (2005), though the age of that event was revised to ~212 ka by Channell and others (2020). Channell and others (2020) do not document a cryptochron near 135 ka.

3. The next oldest example of excursional remanent direction involves multiple eruptive units distinguished on the geologic map (Downs and others, 2019; Robinson and Downs, 2023), and multiple anomalous directions of magnetization (fig. 9). Sites located in the basalt of Ar

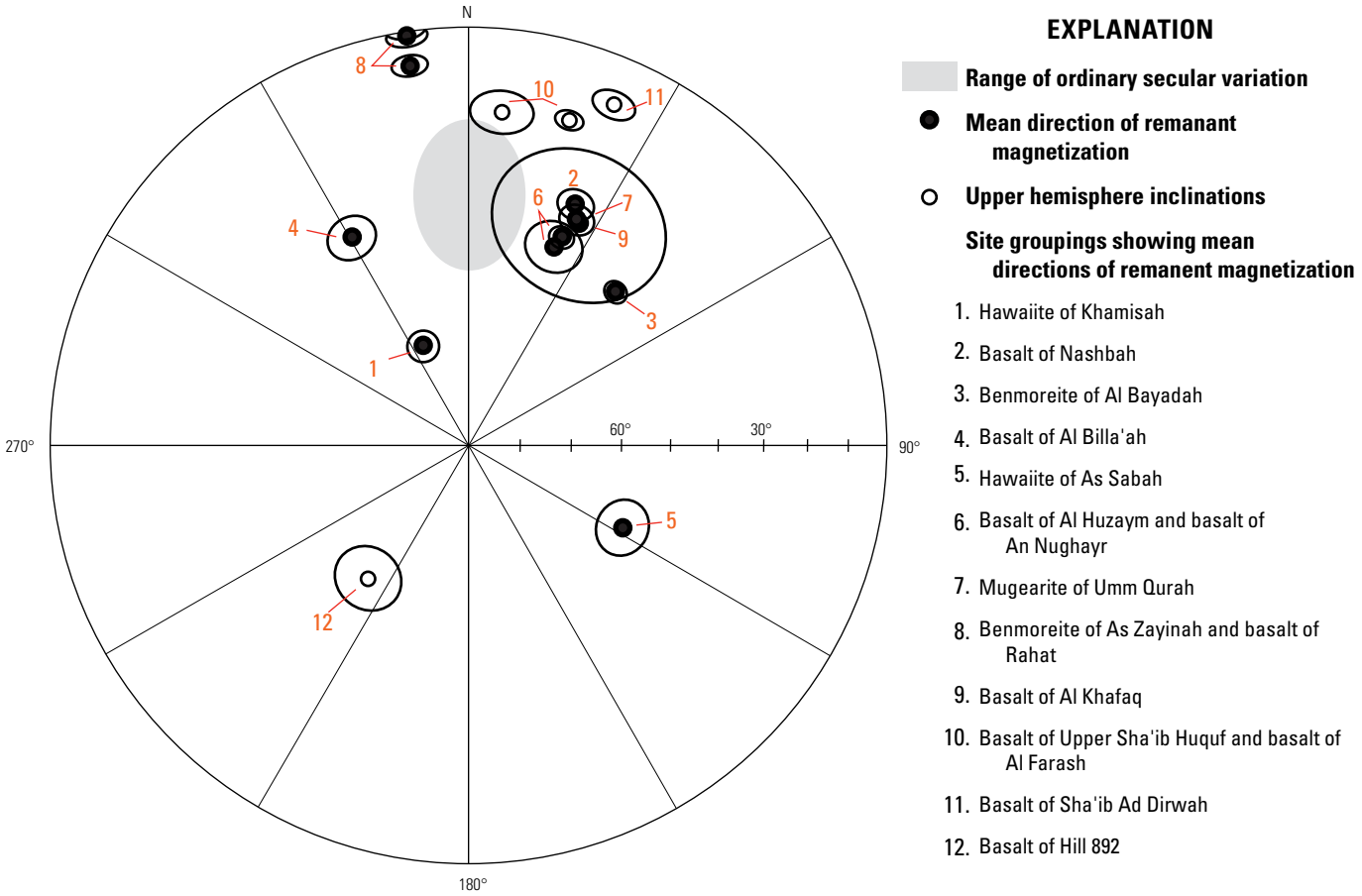

Figure 8. Equal-area plot showing site mean directions of remanent magnetization and enclosing 95 percent confidence envelopes (black ellipses) for sites showing anomalous character outside the range of ordinary secular variation. These remanent directions were acquired during different geomagnetic cryptochrons that occurred during the Brunhes Normal Polarity Chron and earlier during the Matuyama Reversed Polarity Chron.

Table 3. Summary of new $^{40}Ar/^{39}Ar$ ages for three Harrat Rahat lava flows.

[Unit symbols from Downs and others (2019) and Robinson and Downs (2023). All analyses are incremental heating analyses of groundmass separates. Eastings and northings are reported in World Geodetic System of 1984 (WGS 1984) Universal Transverse Mercator Zone 37 north system. Analytical methods are described by Stelten and others (2020, 2023a). Mass discrimination was calculated assuming $^{40}Ar/^{36}Ar_{atmosphere}$ = 298.56±0.31 (Lee and others, 2006). Ages were calculated using the decay constants recommended by Steiger and Jäger (1977). Ages were calculated relative to Bodie Hills sanidine at 9.7946±0.0033 million years ago (Ma) (equivalent to Fish Canyon sanidine at 28.0985±0.0126 Ma). Abbreviations: ka, thousand years before present; σ, standard deviation; MSWD, mean squared weighted deviation; $^{40}Ar/^{36}Ar_i$, isochron intercept; %, percent; °C, degree Celsius]

Unit symbol	Sample	Easting	Northing	Plateau		Isochron			Ar, in % [T range, in °C]
				Age ±1σ (ka)	MSWD	Age ±1σ (ka)	MSWD	$^{40}Ar/^{36}Ar_i$ ±2σ	
bns	R14TRO105	596533	2647955	188.5±15.8	1.98	134.1±24.3	0.66	302.6±3.4	90.9 [600–1,175]
hsb	R17AC159	601694	2676324	349.5±12.1	1.72	271.6±62.9	1.41	306.0±13.3	47.7 [950–1,150]
bgh	R17AC128	582059	2665871	930.2±20.1	0.24	922.0±26.4	0.25	299.3±3.8	90.1 [600–1,150]

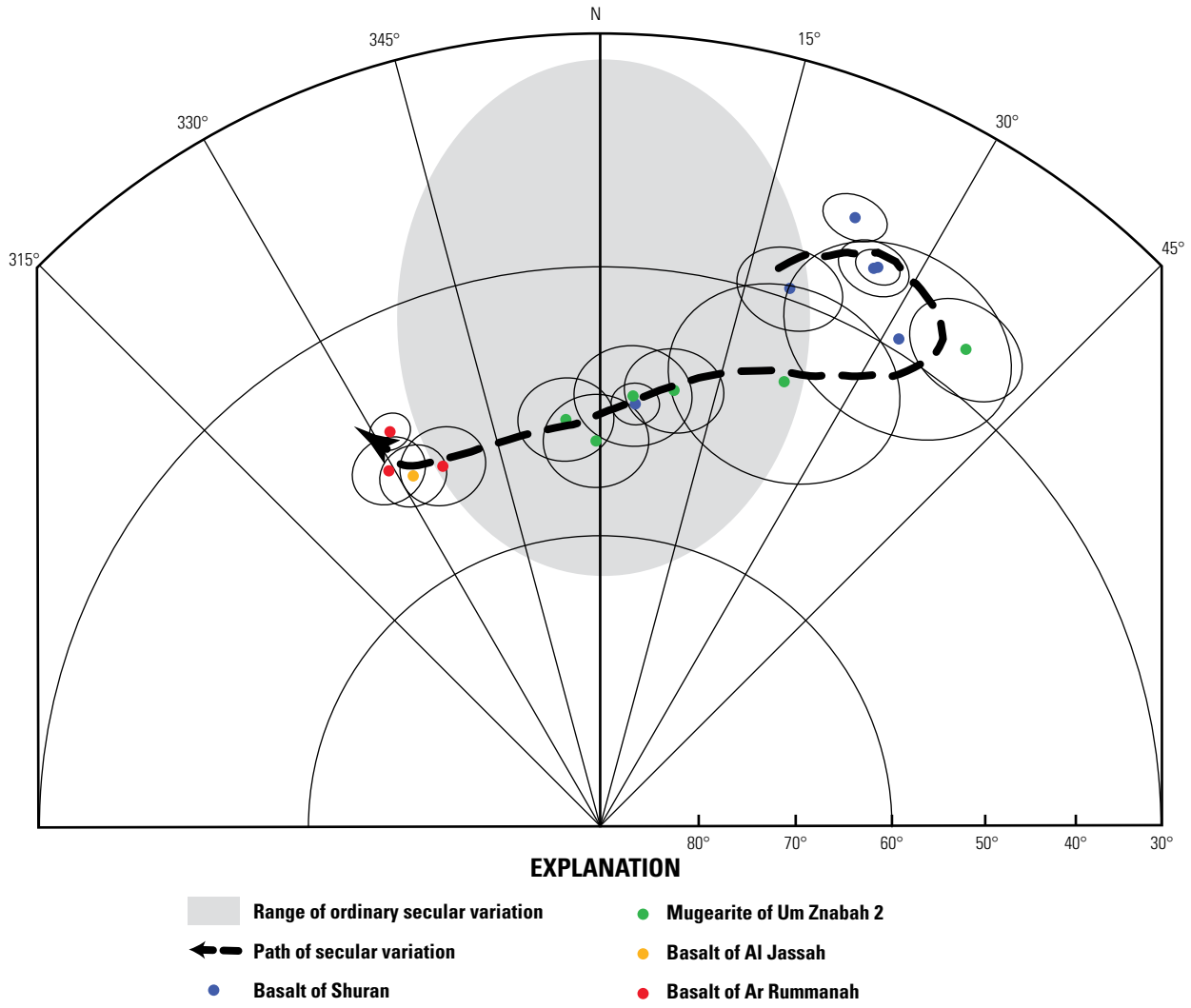

Figure 9. Northern part of a lower hemisphere equal-area plot showing site mean directions of remanent magnetization and enclosing 95 percent confidence envelopes (black ellipses) for sites thought to record sweeping changes in the local magnetic field acquired during the Iceland Basin Cryptochron (190–180 thousand years ago [ka]; Oda, 2005; Channell and others, 2020). The black arrow connects the Harrat Rahat sites in stratigraphic order, showing the path of geomagnetic secular variation. These four units have $^{40}Ar/^{39}Ar$ ages around 193 ka and record the movement of the geomagnetic field during the cryptochron.

Rummanah (unit bru), basalt of Al Jassah (unit bjs), basalt of Shuran (unit bsh), and the mugearite of Um Znabah 2 (unit mz2) record a directional clockwise loop to shallow inclinations and northeasterly declinations, followed by a sweep to steeper inclination and northwesterly declinations. Ordinarily such directional variation would not suggest possible correlation within a brief time interval. However, both the basalt of Shuran and especially the mugearite of Um Znabah 2, record broadly internally changing directions not characteristic of the limited geomagnetic variation during a typical eruptive event. The path and continuity of this rapid magnetic variation becomes evident when the data are plotted together (fig. 9).

4. Two $^{40}Ar/^{39}Ar$ ages are available from units erupted during this reconstructed geomagnetic event. The $^{40}Ar/^{39}Ar$ age for the basalt of Shuran is 191.5±4.2 ka, whereas the $^{40}Ar/^{39}Ar$ age for the mugearite of Um Znabah 2 is 195.9±1.3 ka. These ages are just older than the ~190 ka age suggested for the Iceland Basin Cryptochron (Oda, 2005) and older than the ~188 ka age suggested by Channell and others (2020). The path of geomagnetic secular variation here reconstructed from Harrat Rahat mimics the path of variation discerned from drill core samples documenting the Iceland Basin Cryptochron in the northern Atlantic Ocean (Channell, 2014).

5. The benmoreite of Al Bayadah (unit oba) records an excursional remanent magnetic direction with somewhat steep inclination, far easterly declination, and a colatitude value of 39° (fig. 8). The $^{40}Ar/^{39}Ar$ plateau age for the benmoreite of Al Bayadah is 242.8±2.4 ka, which correlates well to a cryptochron named marine isotope stage (MIS) 7e at around 238 ka (Channell and others, 2020). The plateau age is somewhat younger than the Fram Strait Cryptochron (265–255 ka) of Oda (2005). The $^{40}Ar/^{36}Ar$ isochron intercept value is 291.7±4.2, and although it overlaps with, it is significantly lower than, the $^{40}Ar/^{36}Ar$ atmospheric value of 295.5 used for that age measurement experiment. The isochron age of 255.5±6.8 ka (Stelten and others, 2020, 2023a) probably better represents the age of this unit.

6. The basalt of Al Billa'ah (unit bli) records an excursional remanent magnetic direction with ordinary inclination, but far westerly declination and a colatitude value of 27° (fig. 8). An $^{40}Ar/^{39}Ar$ age was not obtained for this basalt, but an age on an overlying lava flow indicates it is older than 217 ka. Stelten and others (2020, 2023a) place this unit in the oldest part of eruptive stage 6 for Harrat Rahat (Downs and others, 2019; Robinson and Downs, 2023), and thus near 260 ka. Although it may have erupted during the Pringle Falls Cryptochron at 238–215 ka (Channell and others, 2020), it is more likely that the basalt of Al Billa'ah also correlates with the Fram Strait Cryptochron (265–255 ka) of Oda (2005).

7. The hawaiite of As Sabah (unit hsb) records the most anomalous normal polarity remanent magnetic direction obtained from lava flows of northern Harrat Rahat. Although its inclination value is somewhat steep at 56°, the declination value is 118° and isolated in the southeast quadrant of figure 8. The $^{40}Ar/^{39}Ar$ age experiment performed on a sample from this unit yielded a plateau age of 349.7±12.1 ka, whereas the isochron age is imprecisely determined at 271.6±62.9 ka. Only 48 percent of the ^{39}Ar release was used in calculating these ages. The imprecise isochron age involves fewer assumptions than the plateau age, so we prefer that interpretation. Although the uncertainty in the isochron age allows correlation of this unit to the Pringle Falls and Fram Strait Cryptochrons, the more likely tie is with the Kolbeinsey Ridge Cryptochron (290–280 ka) of Oda (2005). Channell and others (2020) report the Portuguese Orphan Cryptochron at ~286 ka that correlates well with the imprecise isochron age.

8. The basalt of Al Huzaym (unit bhu) records an excursional remanent magnetic direction with ordinary inclination, far easterly declination, and colatitude values as low as 23° for most of the sites composing its mean direction (fig. 8). The $^{40}Ar/^{39}Ar$ age for this basalt is 285.1±6.6 ka, which overlaps with the range of the Kolbeinsey Ridge Cryptochron (Oda, 2005) or the Portuguese Orphan Cryptochron of Channell and others (2020). The remanent magnetic direction for the nearby basalt of An Nughayr (unit bau) is at the margin of ordinary secular variation and nearly identical to that of the basalt of Al Huzaym, thus it is likely it also erupted during the Kolbeinsey Ridge Cryptochron.

9. The mugearite of Umm Qurah (unit muq) records an excursional remanent magnetic direction with slightly shallow inclination, far easterly declination, and a colatitude value of 23° (fig. 8). The $^{40}Ar/^{39}Ar$ isochron age for this unit is 385.6±12.6 ka, suggesting correlation with either the Levantine Cryptochron (370–360 ka) or the Weinen Cryptochron (420–400 ka) of Oda (2005). Although the $^{40}Ar/^{36}Ar$ isochron intercept is high and somewhat imprecise, the plateau age of 402.6±3.4 ka would strengthen the tie to the Weinen Cryptochron. A possible correlation suggested from Channell and others (2020) would be the Bermuda Cryptochron at ~412 ka, although that appears too old.

10. The benmoreite of As Zayinah (unit ozy) and the basalt of Rahat (unit brh) share excursional remanent magnetic directions with very shallow inclinations, north-northwesterly declinations, and colatitudes ranging from 21° to 63° (fig. 8). They also share similar $^{40}Ar/^{39}Ar$ ages of 418.8±1.9 ka for the benmoreite of As Zayinah and 411.5±5.9 ka for the basalt of Rahat. These ages overlap with the range of the Weinen Cryptochron (Oda, 2005) or the Bermuda Cryptochron of Channell and others (2020).

11. The basalt of Al Khafaq (unit bkf) records an excursional remanent magnetic direction with ordinary inclination, far easterly declination, and a colatitude of 24° (fig. 8). There is no $^{40}Ar/^{39}Ar$ age for this basalt and it is overlain by three lava flows much younger than its age assessment of 570 to 460 ka (eruptive stage 10 of Downs and others, 2019; Robinson and Downs, 2023). Within that age range, the basalt of Al Khafaq may have temporal ties to the West Eifel, Calabrian Ridge 2, or Emperor/Big Lost Cryptochrons of Oda (2005), or the Orphan Knoll, Big Lost, or La Palma Cryptochrons of Channell and others (2020).

12. The basalt of Upper Sha‘ib Huquf (unit buph) and the basalt of Al Farash (unit bfa) both record excursional remanent magnetic directions with shallow reversed inclinations, easterly declinations, and colatitudes of 38° and 35°, respectively (fig. 8). The $^{40}Ar/^{39}Ar$ age for the basalt of Upper Sha’ib Huquf is 510.8±29.4 ka and lies within the range of the West Eifel Cryptochron (510–500 ka; Oda, 2005) or the Orphan Knoll Cryptochron (~495 ka; Channell and others, 2020), which is likely recorded by both units owing to their similar anomalous remanent magnetic directions.

13. The basalt of Sha‘ib Ad Dirwah (unit bsd) records an excursional remanent magnetic direction with shallow reversed polarity inclination, far easterly declination, and a colatitude of 38° (fig. 8). The $^{40}Ar/^{39}Ar$ age for this unit is 584.5±10.4 ka, which lies within the range of the Calabrian Ridge 3 Cryptochron (605–580 ka; Oda, 2005) or the La Palma Cryptochron (~580 ka; Channell and others, 2020).

14. The basalt of Hill 892 (unit bh89) records an excursional remanent magnetic direction with steep reversed polarity inclination and declination to the southwest (fig. 8). The $^{40}Ar/^{39}Ar$ age for this unit is 1,014.0±14.0 ka, an age which overlaps with both the onset of the Jaramillo Normal Polarity Subchron and the Cobb Mountain Cryptochron (~1.2 mega-annum [million years ago] at 2σ uncertainty) of the Matuyama Reversed Polarity Chron. Consequently, the colatitude value of the VGP for the basalt of Hill 892 is either 146° if it erupted during the transition into the Jaramillo Subchron or 34° if it erupted during the later part of the Matuyama Chron. The $^{40}Ar/^{39}Ar$ isochron age of 988±42 ka may best determine when the anomalous remanent direction from the basalt of Hill 892 was acquired. The measured $^{40}Ar/^{36}Ar$ intercept value of 299.9±4.6 is slightly higher than the atmospheric value of 298.6 assumed for this age measurement experiment (Stelten and others, 2020, 2023a). If the 988 ka age is correct, then the eruption of this unit correlates well with the termination of the Jaramillo Subchron at 990 ka.

Conclusions

This study demonstrates the utility of combining paleomagnetic field studies with geologic mapping and geochronology. Where the age dating is limited or imprecise, paleomagnetic data in the context of the known polarity time scale (Oda, 2005; Channell and others, 2020) can provide both geologic map unit correlation and chronologic constraints. Paleomagnetic field studies of northern Harrat Rahat demonstrate that individual eruptive deposits typically preserve single mean remanent magnetic directions. These directions were used in combination with archaeomagnetic data to evaluate assigned ages of Holocene and older lava flows, showing that the direction of remanent magnetization for the basalt of Al Labah is consistent with its known eruption in 1256 C.E. (654 in the year of the Hijra [A.H.]). In contrast, the direction of remanent magnetization of four cinder cones and small lava flows of the basalt of Al Du’aythah in Al Madīnah’s western suburb is inconsistent with their eruption in 641 C.E. (20 A.H.), which was speculated by previous researchers. A ^{36}Cl surface-exposure age near 13 ka for those cinder cones and flows confirms their eruption shortly before the Holocene. Paleomagnetic measurements from the large, young-appearing Habir and Qidr basalt flows on the west slope of Harrat Khaybar, when combined with ^{36}Cl surface-exposure ages, are consistent with its eruption in 641 C.E., potentially reconciling the brief note of an eruption that year somewher in the greater Al Madīnah region (Al-Samhūdī, 1488). Paleomagnetic results also indicate multiple periods of temporally clustered eruptions in northern Harrat Rahat, consistent with a mixed-exponential probability description of repose periods between eruptions (Stelten and others, 2023a). The practical implication of the mixed exponential is that, although low in absolute probability, the chances of an eruption are elevated in the first few hundred years after a prior eruption, and that the successor eruption(s) need not be close to or of the same magma type or character as the preceeding eruption. Enough time has elapsed since the 1256 C.E. eruption, however, that the estimated present eruption probability is indistinguishable from the long-term value (Stelten and others, 2023a). Additionally, we identify 13 eruptive episodes when the local geomagnetic field exceeded the limits of ordinary secular variation. These observations were used to augment, confirm, and improve $^{40}Ar/^{39}Ar$ age assignments.

Acknowledgments

This paleomagnetic field study would not have been possible without the fiscal and material support of the Saudi Geological Survey (SGS) under the Presidency of Dr. Zohair A.H. Nawab. Numerous members of the SGS assisted in the field, as liaisons with Saudi residents, and as guides to the

extent and beauty of Harrat Rahat, and their contributions were invaluable. Peer reviews by Drs. Julie Donnelly-Nolan and Charles Bacon and editorial comments by Dr. Monica Erdman, Mitchell Phillips, and John Mark Brigham greatly improved the text and are greatly appreciated.

References Cited

Al-Samhūdī, A.B.A.A., 1488 [edited and reprinted in 2001], Wafāʿ al-Wafāʿ bi Akhbār Dār al-Muṣṭafā: London, Al-Furqān Islamic Heritage Foundation, 2,615 p.

Burton, R.F., 1879, The land of the Midian (revisited), vol. II: London, Kegan Paul & Co., 358 p.

Camp, V.E., Hooper, P.R., Roobol, M.J., and White, D.L., 1987, The Madinah eruption, Saudi Arabia—Magma mixing and simultaneous extrusion of three basaltic chemical types: Bulletin of Volcanology, v. 49, p. 498–508.

Camp, V.E., and Roobol, M.J., 1989, The Arabian continental alkali basalt province; Part I— Evolution of Harrat Rahat, Kingdom of Saudi Arabia: Geological Society of America Bulletin, v. 101, p. 71–95.

Camp, V.E., and Roobol, M.J., 1991, Geologic map of the Cenozoic lava field of Harrat Rahat, Kingdom of Saudi Arabia: Saudi Arabian Deputy Ministry for Mineral Resources Geoscience Map GM-123, scale 1:250,000, 37 p.

Channell, J.E.T., 2014, The Iceland Basin excursion—Age, duration, and excursion field geometry: Geochemistry, Geophysics, Geosystems, v. 15, p. 4920–4935, https://doi.org/10.1002/2014GC005564.

Channell, J.E.T., 2020, Timing of Quaternary geomagnetic reversals and excursions in volcanic and sedimentary archives: Quaternary Science Reviews, v. 228, 24 p., https://doi.org/10.1016/j.quascirev.2019.106114.

Coleman, R.G., Gregory, R.T., and Brown, G.F., 1983, Cenozoic volcanic rocks of Saudi Arabia: U.S. Geological Survey Open-File Report 83–788, 82 p., https://doi.org/10.3133/ofr83788.

Dalrymple, G.B., Alexander, E.C., Lanphere, M.A., and Kraker, G.P., 1981, Irradiation of samples for $^{40}Ar/^{39}Ar$ dating using the Geological Survey TRIGA reactor: U.S. Geological Survey Professional Paper 1176, 55 p., https://doi.org/10.3133/pp1176.

Desilets, D., Zreda, M., Almasi, P.F., and Elmore, D., 2006, Determination of cosmogenic ^{36}Cl in rocks by isotope dilution—Innovations, validation and error propagation: Chemical Geology, v. 233, p. 185–195, https://doi.org/10.1016/j.chemgeo.2006.03.001.

Dietterich, H.R., Downs, D.T., Stelten, M.E., and Zahran, H., 2018, Reconstructing lava flow emplacement histories within the northernmost part of the Harrat Rahat volcanic field, Kingdom of Saudi Arabia: Bulletin of Volcanology, v. 80, p. 1–23.

Downs, D.T., 2019, Major- and trace-element chemical analyses of rocks from the northern Harrat Rahat volcanic field and surrounding area, Kingdom of Saudi Arabia: U.S. Geological Survey data release, https://doi.org/10.5066/P91HL91C.

Downs, D.T., Robinson, J.E., Stelten, M.E., Champion, D.E., Dietterich, H.R., Sisson, T.W., Zahran, H., Hassan, K., and Shawali, J., 2019, Geologic map of the northern Harrat Rahat volcanic field, Kingdom of Saudi Arabia: U.S. Geological Survey Scientific Investigations Map 3428 [also released as Saudi Geological Survey Special Report SGS–SP–2019–2], 65 p., 4 sheets, scales 1:75,000, 1:25,000, https://doi.org/10.3133/sim3428.

Downs, D.T., Stelten, M.E., Champion, D.E., Dietterich, H.R., Hassan, K., and Shawali, J., 2023, Eruptive history within the vicinity of Al Madīnah in northern Harrat Rahat, Kingdom of Saudi Arabia, chap. C *of* Sisson, T.W., Calvert, A.T., and Mooney, W.D., eds., Active volcanism on the Arabian Shield—Geology, volcanology, and geophysics of northern Harrat Rahat and vicinity, Kingdom of Saudi Arabia: U.S. Geological Survey Professional Paper 1862 [also released as Saudi Geological Survey Special Report SGS–SP–2021–1], 41 p., https://doi.org/10.3133/pp1862C.

Downs, D.T., Stelten, M.E., Champion, D.E., Dietterich, H.R., Nawab, Z., Zahran, H., Hassan, K., and Shawali, J., 2018, Volcanic history of the northernmost part of the Harrat Rahat volcanic field, Saudi Arabia: Geosphere, v. 14, no. 3, p. 1253–1282, https://doi.org/10.1130/GES01625.1.

Fleck, R.J., Calvert, A.T., Coble, M.A., Wooden, J.L., Hodges, K., Hayden, L.A., van Soest, M.C., du Bray, E.A., and John, D.A., 2019, Characterization of the rhyolite of Bodie Hills and $^{40}Ar/^{39}Ar$ intercalibration of Ar mineral standards: Chemical Geology, v. 525, p. 282–302.

Gauss, C.F, 1838, Resultate as den Beobachtungen des magnetischen Vereins im Jahre 1837 [On a new instrument for the direct observation of the changes in the intensity of horizontal portion of the terrestrial magnetic force]: Scientific Memoirs, v. 2, p. 252–267.

Kirschvink, J.L., 1980, The least-square line and plane and the analysis of paleomagnetic data: Geophysical Journal International, v. 62, p. 699–718.

Kovacheva, M., 1997, Archaeomagnetic database from Bulgaria—The last 8,000 years: Physics of the Earth and Planetary Interiors, v. 102, p. 145–151.

Kovacheva, K, Boyadziev, Y., Kostadinova-Avramova, M., Jordanova, N., and Donadini, F., 2009, Updated archaeomagnetic data set of the past 8 millennia from the Sofia laboratory, Bulgaria: Geochemistry, Geophysics, Geosystems, v. 10, no. 5, 6 p. https://doi.org/10.1029/2008GC002347.

Laj, C., Guillou, H., and Kissel, C., 2014, Dynamics of the Earth magnetic field in the 10–75 kyr period comprising the Laschamp and Mono Lake excursions—New results from the French Chaîne des Puys in a global perspective: Earth and Planetary Science Letters, v. 387, p. 184–197, https://doi.org/10.1016/j.epsl.2013.11.031.

Lal, D., 1991, Cosmic ray labeling of erosion surfaces—in situ nuclide production rates and erosion models: Earth and Planetary Science Letters, v. 104, p. 424–439, https://doi.org/10.1016/0012-821X(91)90220-C.

Lee, J.Y., Marti, K., Severinghaus, J.P., Kawamura, K., Yoo, H.S., Lee, J.B., and Kim, J.S., 2006, A redetermination of the isotopic abundances of atmospheric Ar: Geochemica Cosmochemica Acta, v. 70, p. 4507–4512.

Leonard, G.S., Calvert, A.C., Hopkins, J.L., Wilson, C.J.N., Smid, E.R., Lindsey, J.M., and Champion, D.E., 2017, High-precision $^{40}Ar/^{39}Ar$ dating of Quaternary basalts from Auckland Volcanic Field, New Zealand, with implications for eruption rates and paleomagnetic correlations: Journal of Volcanology and Geothermal Resources, v. 343, p. 60–74.

Marcaida, M., Vazquez, J.A., Stelten, M.E., and Miller, J.S., 2019, Constraining the early eruptive history of the Mono Craters rhyolites, California, based on $^{238}U–^{230}Th$ isochron dating of their explosive and effusive products: Geochemistry, Geophysics, Geosystems, v. 20, p. 1539–1556, https://doi.org/10.1029/2018GC008052.

Marrero, S.M., Phillips, F.M., Borchers, B., Lifton, N., Aumer, R., and Balco, G., 2016, Cosmogenic nuclide systematics and the CRONUScalc program: Quaternary Geochronology, v. 31, p. 160–187, https://doi.org/10.1016/j.quageo.2015.09.005.

McElhinny, M.W., 1973, Paleomagnetism and plate tectonics: Cambridge, United Kingdom, University Press, 368 p.

Moufti, M.R.H., 1985, The geology of Harrat Al Madinah volcanic field, Harrat Rahat, Saudi Arabia: University of Lancaster, Ph.D. dissertation, 407 p.

Moufti, M.R., and Németh, K., 2016, Geoheritage of volcanic harrats in Saudi Arabia: Switzerland, Springer, 194 p.

Murcia, H., Németh, K., El-Masry, N.N., Lindsay, J.M., Moufti, M.R.H., Wameyo, P., Cronin, S.J., Smith, I.E.M., and Kereszturi, G., 2015, The Al-Du'aythah volcanic cones, Al-Madinah City—Implications for volcanic hazards in northern Harrat Rahat, Kingdom of Saudi Arabia: Bulletin of Volcanology, v. 77, 19 p.

Murcia, H., Lindsay, J.M., Németh, K., Smith, I.E.M., Cronin, S.J., Moufti, M.R.H., El-Masry, N.N., and Niedermann, S., 2016, Geology and geochemistry of late Quaternary volcanism in northern Harrat Rahat, Kingdom of Saudi Arabia—Implications for eruption dynamics, regional stratigraphy, and magma evolution, *in* Németh, K., Carrasco-Núñez, G., Aranda-Gómez, J.J., and Smith, I.E.M., eds., Monogenetic volcanism: Geological Society of London Special Publication 446, p. 173–204, https://doi.org/10.1144/SP446.2.

Oda, H., 2005, [Recurrent geomagnetic excursions—A review for the Brunhes normal polarity chron]: Japanese Journal of Geography, v. 114, p. 174–193.

Principe, C., Tanguy, J.C., Arrighi, S., Paiotti, A., Le Goff, M., and Zoppi, U., 2004, Chronology of Vesuvius' activity from A.D. 79 to 1631 based on archeomagnetism of lavas and historical sources: Bulletin of Volcanology, v. 66, p. 703–724.

Robinson, J.E., and Downs, D.T., 2023, Overview of the Cenozoic geology of the northern Harrat Rahat volcanic field, Kingdom of Saudi Arabia, chap. R *of* Sisson, T.W., Calvert, A.T., and Mooney, W.D., eds., Active volcanism on the Arabian Shield—Geology, volcanology, and geophysics of northern Harrat Rahat and vicinity, Kingdom of Saudi Arabia: U.S. Geological Survey Professional Paper 1862 [also released as Saudi Geological Survey Special Report SGS–SP–2021–1], 20 p., scale 1:100,000, https://doi.org/10.3133/pp1862R.

Roobol, M.J., and Camp, V.E., 1991, Geology of the Cenozoic lava fields of Harrats Khaybar, Ithnayn and Kura, Kingdom of Saudi Arabia: Saudi Arabian Directorate General of Mineral Resources Geoscience Map GM-131, scale 1:250,000.

Shaar, R., Hassul, E., Raphael, K., Ebert, Y., Segal, Y., Eden, I., Vaknin, Y., Marco, S., Nowaczyk, N.R., Chauvin, A., and Agnon, A., 2018, The first catalog of archaeomagnetic directions from Israel with 4,000 years of geomagnetic secular variations: Frontiers in Earth Science, 14 p., https://doi.org/10.3389/feart.2018.00164.

Steiger, R.H. and Jäger, E., 1977, Subcommission on geochronology—Convention on the use of decay constants in geo- and cosmochronology: Earth and Planetary Science Letters, v. 36, p. 359–362.

Stelten, M.E., 2021, Ar isotope data for volcanic rocks from the northern Harrat Rahat volcanic field and surrounding area, Kingdom of Saudi Arabia: U.S. Geological Survey data release, https://doi.org/10.5066/P92FB6AQ.

Stelten, M.E., Downs, D.T., Champion, D.E., Dietterich, H.R., Calvert, A.T., Sisson, T.W., Mahood, G.A., and Zahran, H., 2020, The timing and compositional evolution of volcanism within northern Harrat Rahat, Kingdom of Saudi Arabia: Geological Society of America Bulletin, v. 132, p. 1381–1403, https://doi.org/10.1130/B35337.1.

Stelten, M.E., Downs, D.T., Champion, D.E., Dietterich, H.R., Calvert, A.T., Sisson, T.W., Mahood, G.A., and Zahran, H.M., 2023a, Eruptive history of northern Harrat Rahat—Volume, timing, and composition of volcanism over the past 1.2 million years, chap. D *of* Sisson, T.W., Calvert, A.T., and Mooney, W.D., eds., Active volcanism on the Arabian Shield—Geology, volcanology, and geophysics of northern Harrat Rahat and vicinity, Kingdom of Saudi Arabia: U.S. Geological Survey Professional Paper 1862 [also released as Saudi Geological Survey Special Report SGS–SP–2021–1], 46 p., https://doi.org/10.3133/pp1862D.

Stelten, M.E., Downs, D.T., Dietterich, H.R., Mahood, G.A., Calvert, A.T., Sisson, T.W., Witter, M.R., Zahran, H.M., and Shawali, J., 2023b, The duration and characteristics of magmatic differentiation from basalt to trachyte within the Matan volcanic center, northern Harrat Rahat, Kingdom of Saudi Arabia, chap. F *of* Sisson, T.W., Calvert, A.T., and Mooney, W.D., eds., Active volcanism on the Arabian Shield—Geology, volcanology, and geophysics of northern Harrat Rahat and vicinity, Kingdom of Saudi Arabia: U.S. Geological Survey Professional Paper 1862 [also released as Saudi Geological Survey Special Report SGS–SP–2021–1], 56 p., https://doi.org/10.3133/pp1862F.

Stelten, M.E., Downs, D.T., Dietterich, H.R., Mahood, G.A., Calvert, A.T., Sisson, T.W., Zahran, H., and Shawali, J., 2018, Timescales of magmatic differentiation from alkali basalt to trachyte within the Harrat Rahat volcanic field, Kingdom of Saudi Arabia: Contributions to Mineralogy and Petrology, v. 173, 17 p., https://doi.org/10.1007/s00410-018-1495-9.

Stern, R.J., and Johnson, P., 2010, Continental lithosphere of the Arabian Plate—A geologic, petrologic, and geophysical synthesis: Earth-Science Reviews, v. 101, no. 1–2, p. 29–67, https://doi-org.usgslibrary.idm.oclc.org/10.1016/j.earscirev.2010.01.002.

Stone, J.O., 2000, Air pressure and cosmogenic isotope production: Journal of Geophysical Research Solid Earth, v. 105, p. 23753–23759, https://doi.org/10.1029/2000JB900181.

Taggart, J.E., Jr., ed., 2002, Analytical methods for chemical analysis of geologic and other materials, U.S. Geological Survey: U.S. Geological Survey Open-File Report 02–223, 20 p., https://doi.org/10.3133/ofr02223.

Tanguy, J.C., Condomines, M., Le Goff, M., Chillemi, V., La Delfa, S., and Patane, G., 2007, Mount Etna eruptions of the last 2,750 years—Revised chronology and location through archaeomagnetic and ^{226}Ra-^{230}Th dating: Bulletin of Volcanology, 29 p., https://doi.org/10.1007/s00445-007-0121-x.

Tanguy, J.C., Le Goff, M., Principe, C., Arrighi, S., Chillemi, V., Paiotti, A., La Delfa, S., and Patane, G., 2003, Archaeomagnetic dating of Mediterranean volcanics of the last 2100 years—Validity and limits: Earth and Planetary Science Letters, v. 211, p. 111–124.

Tema, E., Hedley, I., and Lanos, P., 2006, Archeomagnetism in Italy—A compilation of data including new results and a preliminary Italian secular variation curve: Geophysical Journal International, v. 167, p. 1160–1171.

Verosub, K.L., and Banerjee, S.K., 1977, Geomagnetic excursions and their paleomagnetic record: Reviews of Geophysics and Space Physics, v. 15, p. 145–155.

Vigliotti, L., 2006, Secular variation record of the Earth's magnetic field in Italy during the Holocene—Constraints for the construction of a master curve: Geophysical Journal International, v. 16, https://doi.org/10.1111/j.1365-246X.2005.02785.x.

Moffett Field Publishing Service Center, California
Manuscript approved June 27, 2022
Edited by Mitchell Phillips and John Mark Brigham
Layout and design by Kimber Petersen
Illustration support by Katie Sullivan

USGS

Champion and others—**Paleomagnetism of the Harrat Rahat Volcanic Field—Geologic Units and Geomagnetic Cryptochrons**—Professional Paper 1862–H

ISSN 1044-9612 (print)
ISSN 2330-7102 (online)
https://doi.org/10.3133/pp1862H